Archives of Computational Methods in Engineering (2020) 27:805–830
https://doi.org/10.1007/s11831-019-09331-1

ORIGINAL PAPER

From Topology Optimization Design to Additive Manufacturing: Today's Success and Tomorrow's Roadmap

Liang Meng[1] · Weihong Zhang[1] · Dongliang Quan[2] · Guanghui Shi[2] · Lei Tang[1] · Yuliang Hou[3] · Piotr Breitkopf[4] · Jihong Zhu[1,5] · Tong Gao[1,5]

Received: 15 November 2018 / Accepted: 25 February 2019 / Published online: 7 March 2019

Abstract
This work grew out of rapid developments of topology optimization approaches and emerging industry trends of "3D printing" techniques, the latter bridging to a large extent the gap between innovative design and advanced manufacturing. In the present work, we first make an *application-oriented* review of topology optimization approaches in an attempt to illustrate their efficacy in the design of high-performance structures. Subsequently, a broad panorama of additive manufacturing is provided with a particular interest in its application in the automotive and the aerospace sectors. Taking an aerospace bracket as an example, we further go through an entire procedure from topology optimization design to additive manufacturing, then to performance verification. In the interest of cultivating a long-term partnership upon this combination, we finally examine, in face of present and near future, limitations of additive manufacturing in the *loss of geometric accuracy* and *performance deterioration*, and provide a roadmap for future work.

1 General Introduction

In seeking stiffness-, strength- and endurance-fulfilled design on a component level, structural optimization has long been practiced and was proved to be efficient in designing sustainable products [1–3]. Topology optimization (TO), within one of the three sub-fields of structural optimization (the other two are size and shape optimization), is mostly employed in the early stage of structural design. This conceptual design, always leading to weight-competitive structures, seeks for the best distribution of material by creating, merging and splitting interior voids during structural evolution. The past decades have witnessed a significant development of TO in both theoretical and practical aspects [4–6], and dedicated review work can be found in [7–10].

Conventionally, an innovative TO-based Design for Manufacturing (DfM) shall comprise four stages as illustrated in Fig. 1 (upper graph). A mathematical model is first built to interpret the blueprint of the mechanical structure/system, the primary objective of which is to define the admissible domain constraining the structural evolution. Various design requirements are then carefully chosen at the second stage to cater for both high structural performance and potential manufacturing restrictions. At the third stage, a reconstruction of the optimal design is performed with CAD primitives to avoid the too "*organic*" features issued from TO. This reconstruction, however, inevitably entails a compromise between structural manufacturability and optimal performance. As such, a re-analysis procedure is necessitated to ensure that none of the constraints (i.e., design requirements) are violated before the part is finally manufactured at the final stage.

Despite extensive literature on TO-based structural design, most if not all of the research work can be included in the above-mentioned four-stage framework. For example,

✉ Tong Gao
gaotong@nwpu.edu.cn

Weihong Zhang
zhangwh@nwpu.edu.cn

1 State IJR Center of Aerospace Design and Additive Manufacturing, Northwestern Polytechnical University, Xi'an 710072, China

2 Beijing Aerospace Technology Institute, Beijing 100074, China

3 School of Mechanical Engineering, Zhengzhou University, Zhengzhou 450001, China

4 Laboratoire Roberval, UMR 7337 UTC-CNRS, Sorbonne Universités, Université de Technologie de Compiègne, 60200 Compiègne, France

5 Institute of Intelligence Material and Structure, Unmanned System Technologies, Northwestern Polytechnical University, Xi'an 710072, China

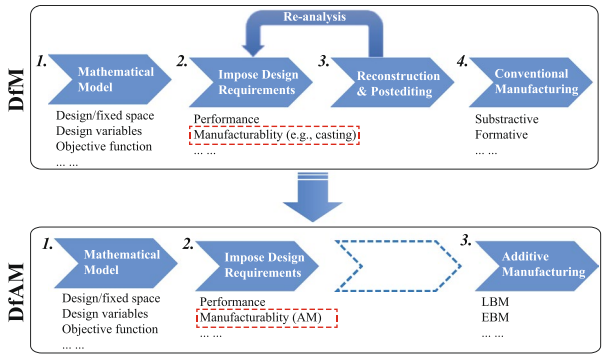

Fig. 1 An ongoing shift from Design for Manufacturing (upper graph) towards Design for Additive Manufacturing (lower graph)

concerning the first stage, the optimization of a single mechanical element (within the macroscopic scale) has attracted a great deal of attention [11], while some others were interested in the design of multi-component systems where the component layout and the supporting structural topology were optimized simultaneously [12–14]. At the second stage, structural performances and manufacturing-associated constraints are thus far two driving concerns in choosing design requirements. On the one hand, a handful of research work has been devoted to seeking for the optimal designs of high-performance structures. Representative work covers various topology optimizations under the guidance of structural stiffness [15, 16], static strength [1, 17, 18] and dynamic responses [19], to name only a few. On the other hand, some effort has also been devoted to rendering the design manufacturable given the inadequacy of conventional manufacturing methods. In this regard, diverse formulations have been developed to take into account issues such as length scale control [20–22] and parting direction [23–25]. Unfortunately, these measures place significant demands on the operator's experience, and not all solutions are mature enough for industrial applications, at least for the time being [10].

Recently, additive manufacturing (AM), allowing to build 3D as-designed structures in a *layer-by-layer* manner regardless of their complexities, is fast becoming an alternative to conventional fabrication methods such as machining, casting, or the combination of these. With its merits of high flexibility and efficiency, AM has naturally reshaped the definition of DfM, and a paradigm shift towards Design for Additive Manufacturing (DfAM) has been proposed in [26] (Fig. 1 lower graph).

Thus far, the influence of AM on TO has been observed from different perspectives. First and most importantly, the usually time-consuming "*Reconstruction and Posteditting*" stage, and by consequence, the "Re-analysis" in DfM were theoretically avoided in DfAM. We attribute this improvement to the unprecedented high flexibility of AM in realizing the as-designed proposal. Secondly, the design model involved in the first stage is becoming more and more complex, and the design of integrated functional part has henceforth turned practicable. Finally, spurred on by the ability of AM in printing features down to micro-scale, multi-scale topology optimization was undertaken such that the structural performance can be promoted to a higher level [27–31].

Despite being a cutting-edge technique for the fabrication of topologically optimized design, AM was bound to fail in printing certain parts where enclosed voids [32, 33] and overhang features [34, 35] are present. Several research groups have been undertaking work to introduce these newly-arisen manufacturing restrictions as constraints of standard TO problem, in such a way that a seamless transition between the optimal design and the final part fabrication is ensured. Furthermore, it has been reported more than once that the mechanical properties of the as-printed part can be different from that characterizing the raw material [36], making the application of AM in printing critical components questionable. Careful quality control and performance verification appeared thus unavoidable. These above-mentioned issues, more or less addressed in the literature, are still under investigation. It seems therefore particularly timely that a critical review is made to include recent research work since this shift from DfM towards DfAM.

The rest of the work is structured as follows: Sect. 2 recalls various topology optimization methodologies, with a particular interest in benchmark applications in light-weight design; a concise panorama-size review of additive manufacturing is then provided in Sect. 3; we elaborate in Sect. 4 a case study on a critical aerospace part to demonstrate the synergistic effect upon the combination of TO and AM; Sect. 5 finally presents the newly emerged challenges that are being or to be dealt with. Closing remarks are provided in Sect. 6 along with perspectives.

2 Topology Optimization in Structural Design

By redistributing material and modifying accordingly the load carrying path, topology optimization has been primarily employed to design high-performance yet light-weight structures. Its various applications have been reported in particular in the design of auto parts, aircraft and aerospace structures, for which mass constraints are frequently imposed.

This section first devotes to a brief review of different topology optimization methodologies, variations of which are subsequently cited on the basis of engineering constraints considered in practice. In the aim of promoting its popularity in structural design, we also showcase by the end of this section a group of innovative designs issued from TO.

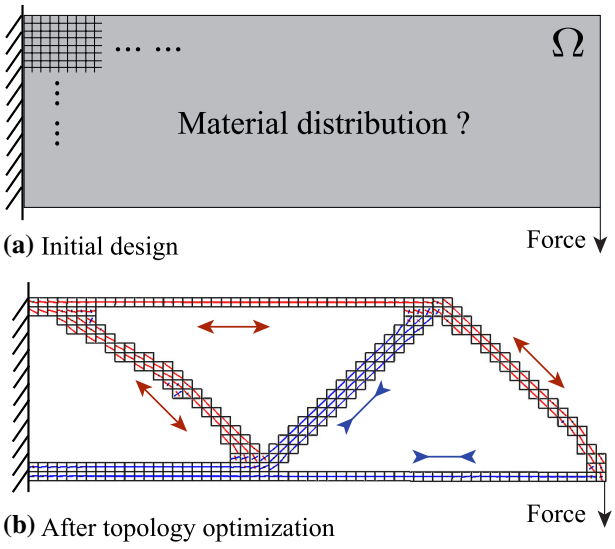

(a) Initial design

(b) After topology optimization

Fig. 2 **a** Topology optimization redistributes material according to the load carrying path. The color code employed in **b** illustrates directions of the principal stress on the beam: blue-compression and red-tension. (Color figure online)

2.1 Topology Optimization Methodologies

Topology optimization, as a pre-processor for shape and size optimization, in its most general setting, should consist of finding out within the design domain Ω the best material distribution that minimizes an objective function f (Fig. 2). The density variable, $\rho(\mathbf{x})$, describing whether there is a material or not at point $\mathbf{x} \in \Omega$, takes either the value 1 or 0, correspondingly. In the pioneering work of Kohn and Strang [37], such problem was stated as a discrete variable formulation

$$\begin{aligned} \arg\min_{\rho} \quad & f(\boldsymbol{u}(\boldsymbol{\rho}), \boldsymbol{\rho}) \\ s.t. \quad & \rho(\mathbf{x}) = 1 \ \text{ or } 0\,, \quad \forall \mathbf{x} \in \Omega \\ & g_j(\boldsymbol{\rho}) \le 0, \quad j = 1, 2 \ldots M \end{aligned} \tag{1}$$

where $f(\cdot)$ in the majority of cases is the compliance of the structure and $\boldsymbol{u}$ is the displacement field. $g_j(\cdot)$ corresponds to M diverse inequality constraints, among which critical mass requirement[1] is the most popular one.

In view of the discrete nature inherent in Eq. (1) and the difficulty in solving it, one may expect to reformulate the problem to a continuous one. Layered structures, porous and periodic composites were introduced in this endeavour. The use of these composites, in essence, moved the *on-off* nature of the problem from the macroscopic scale to a microscopic one. Along with this reformulation, homogenization technique was employed to compute the correlation between the material density and the effective material properties. The design problem appeared consequently as a problem of finding the optimal density-distribution of material [38].

To alleviate the computational complexity, Bendsøe et al. [39] proposed, shortly after the homogenization approach, an interpolation model called SIMP, i.e., Solid Isotropic Material with Penalization. Supposing a power law between the material properties and the density design variables at the elemental level, this model takes the following form

$$E(\rho) = \rho^p E_0 \tag{2}$$

where E_0 is the Young's modulus of solid material, and the penalization parameter, p, generally chosen between 2 and 4, promotes the convergence to a 0–1 solution. In this context, the problem in Eq. (1) is then solved by discretizing the domain Ω into a large number of N finite elements, each associated with a pseudo-density variable ρ_i. An updated formulation with continuous variables was thus proposed

$$\begin{aligned} \arg\min_{\rho} \quad & f(\boldsymbol{u}, \boldsymbol{\rho}), \quad \boldsymbol{\rho} = \left(\rho_1, \rho_2 \cdots \rho_N\right). \\ s.t. \quad & 0 < \rho_i \le 1, \quad i = 1, 2 \ldots N \\ & g_j(\boldsymbol{\rho}) \le 0, \quad j = 1, 2 \ldots M \end{aligned} \tag{3}$$

Through the years, the density-based method has reached a level of maturity, and constitutes the basis for the majority of recent topology optimization literature. Educational papers on this group of methods are found in [40–42], to which readers are referred for more details on TO implementation in MATLAB.

Other than the density-based approach, there exists another branch of TO methodologies which are the heuristic-based evolutionary structural optimization (ESO) approaches.[2] Their very first version was developed in [44] with the intuition to gradually remove inefficient elements from the structure until the pre-defined volume fraction is attained. This method, despite being efficient in some cases, has been criticized for the absence of element restitution. To circumvent this inconvenience, a bi-directional ESO and a soft-killing version were developed and were proved to be more robust and efficient [6, 45]. One is referred to [46] for more details. More recently, the Evolutionary Topology Optimization (ETO) methods using isolines have made a

[1] In engineering practice, the critical mass requirement is considered alternatively as a volumetric constraint in the case of single material formulation.

[2] In view of the discrete nature, Sigmund [43] has categorized the ESO-based approach as a discrete form of the density-based approach.

big step forward, capable of proposing optimal designs with smooth boundaries [47, 48].

Though being straightforward and simple, the above density-based approaches do present certain numerical difficulties, including, among others, mesh-dependency [49], checker-board pattern [50, 51] and local minima [9]. To alleviate these inconveniences, one may employ, on the one hand, numerical techniques such as density and sensitivity filters, and on the other, the level set approach (LSM) as an alternative to density approach. The core spirit of LSM lies in the definition of the structural boundary by the zero-level contour of the level set function (LSF), $\phi(\mathbf{x})$, and the design domain, by convention, as the region where LSF takes positive values. By solving the Hamiton-Jacobi equation, LSF is updated and a new structural boundary can be obtained. The advantages of LSMs over density-based methods lie in the elimination of both intermediate densities and undesired zig-zag boundaries. Nonetheless, challenges such as initial design-dependence and convergence issue do arise, and readers are referred to [52] for more theoretical details.

Most recently, initiated from the LSM and the Multi-Component Layout Design, a new Feature-driven optimization method (FDO) was proposed by Zhou et al. [14]. In addition to the advantages inherited from LSM, the said approach includes fewer design variables, considering both components and structures as designable engineering features [14, 16, 53, 54] . Besides, this approach guaranteed a seamless transition to mainstream CAD systems, viewing that B-splines were adopted to describe the feature boundaries. With these merits, this group of methods has attracted an increasing attention. Independent research carried out in the last years has named the same or similar approaches as Moving Morphable Components (MMC) or Moving Morphable Voids (MMV) methods [55–57].

Aside from the above-mentioned methodologies, topology optimization has also been developed along with other directions, leading to such methods as topological derivatives and phase field. In the aim of tracing the general development of TO methodologies, no further elaboration will be made on these methods and interested readers are referred to [58, 59] for their detailed implementations. Besides, we invite readers to note that, this subsection includes only the research work on the various groups of TO methodologies, while the many papers that employ these methods for solving practical engineering problems and considering diverse design requirements will be cited in the following subsections.

2.2 Popular Design Requirements Considered in TO

Parallel to the development of different TO methods presented in Sect. 2.1, the community has also devoted significant effort in the last decades to promote their applications to a higher level. Though preliminarily employed for the sake of weight-competitive design, TO is now able to deal with more and more performance constraints to withstand demanding environmental, life and reliability requirements.

This short review, not intended to be exhaustive, includes the many related papers with a particular emphasis on the design of critical parts in fulfilling certain performance requirements. In this regard, we decide to follow the classification proposed in [60] to present popular design requirements considered in various static, dynamic, thermo-elastic and manufacturability-related problems.

2.2.1 Static TO Problems

In engineering practice, the stiffest design is always desirable in most if not all cases. To this end, the compliance or the strain energy of the whole structure is generally considered as the objective function to be minimized, or one of the constraints to be satisfied [15, 61]. The displacement magnitudes at given points (usually the points where concentrated force is applied) have analogously been considered to maintain an expected deformation [62–64]. It is noticed that these stiffness-related performance requirements are always considered coupled together with a critical mass limitation.

Other than the stiffness, the strength of the structure is also crucial in practical design. While popular in shape optimization [3, 65, 66], local stress level was controlled with attention in TO as well. However, stress-based topology optimization can be challenging in view of the singularity phenomenon, the local nature of stress constraint, and the highly non-linear stress behavior [67]. Some authors simply took into account potential critical stress constraints over the structure [1, 15], while others integrated these constraints into a single global one [17, 68, 69]. Recently, by using an active-set strategy combined with the dynamic aggregation method, Cai and Zhang [18] obtained better designs of several mechanical parts, in which a large number of stress constraints have been reduced, Fig. 3.

2.2.2 Dynamic TO Problems

Additionally, TO has also been extended to cover dynamic responses, since optimization problems of vibrating structures address a large number of practical applications, particularly in the automotive industry. According to a brief review of available literature, attention has been primarily focused on the optimization of natural frequencies, and the most common design requirements include maximizing a given eigenvalue or achieving a desired separation between eigenvalues. For example, Wu et al. [70] successfully implemented a natural frequencies-based criterion in layout optimization, and [71] separated the first several

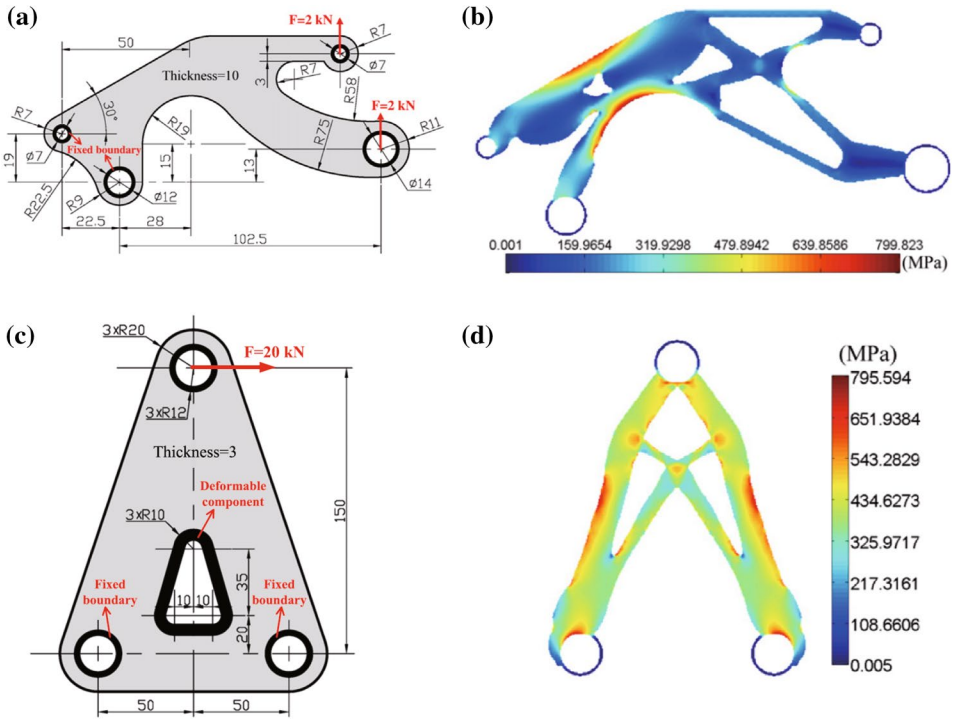

Fig. 3 Minimum compliance designs of **a**, **b** a two-point loading mechanical part and **c**, **d** a bracket with an embedded component, constraining a maximal allowable stress of 800 MPa [18]

eigen-frequencies to improve the quality of resonance in the design of Micro-electro-mechanical resonators.[3]

On the other hand, structural optimization of parts withstanding periodic loadings has also drawn a lot of attention in various practical situations, ranging from portable electric tools to cars and ships. The interest has arisen from the fact that the periodic force is the major source of vibration, and hence noise. On the basis of "dynamic compliance" formulated in [73], Jog et al. [74] remedied the non-positive definite issue in such cases where the driving frequency is slightly higher than the fundamental one, and further developed a global as well as a local measure to bring about a reduction in the vibration level. The proposed global measure has moved the natural frequencies away from the driving frequencies, while the local one was demonstrated to minimize the frequency response amplitude at a given point, by more than an order of magnitude. In responding to the design of structures under *harmonic* excitations, Liu et al. [19] carried out a comparative study on diverse methods, with a particular interest on their computing accuracies and efficiencies. The authors suggested that the Mode Acceleration Method (MAM) is the most favourable method for the optimization problem with harmonic excitation in frequency intervals, Fig. 4. As regards to stationary *random* force excitation problem, Zhang et al. [74] circumvented the non-convergent design pattern resulted from the low computing accuracy for large-scale problems by integrating the Pseudo Excitation Method (PEM) and MAM.

2.2.3 Thermo-Elastic TO Problems

The design of the thermo-elastic structure is recognized as another common issue in the aerospace and the power engineering fields. In this kind of problems, a compromise always needs to be reached between the minimum structural compliance and the maximum strength. In these days, such problems have undergone extensive research, and various criteria have been comparatively studied.

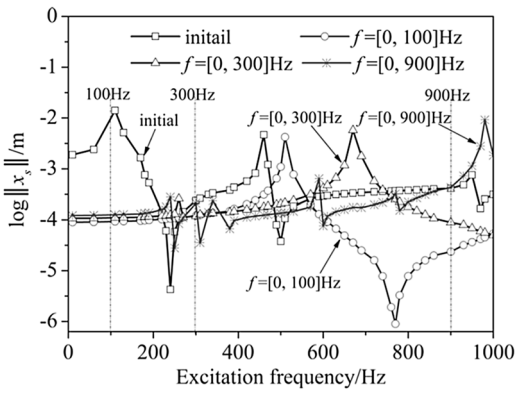

Fig. 4 Displacement amplitudes of the initial and optimized structures under harmonic excitation in different frequency intervals [19]

[3] Please note that the Micro-electro-mechanical system is more popularly known as MEMS.

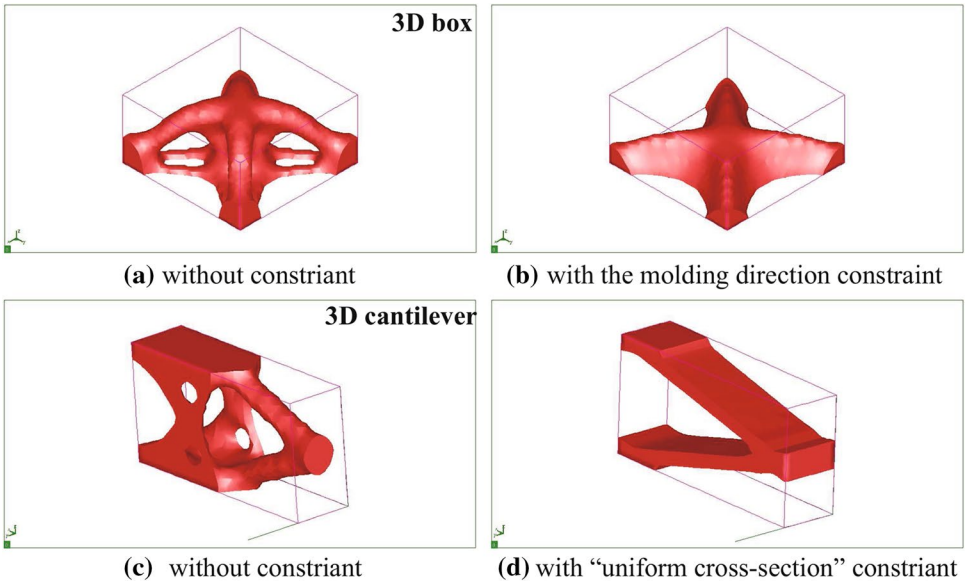

Fig. 5 Different configurations of topologically optimized 3D box and cantilever: **a** and **c** without any manufacturing constraints, **b** and **d** with two types of molding direction constraints [78]

A great majority of pioneering work has followed the practice of static TO design, where the mean compliance of the whole structure has been adopted as design objective [11, 75, 76]. It was demonstrated that the consideration or not of the thermal load might have a strong impact on the final design. This was explained in [76] by the fact that compliance is no longer monotonous with respect to material volume due to the introduction of thermal loads. After a detailed comparative investigation, Zhang et al. [61] pointed out that the mean compliance and the elastic strain energy are inequivalent criteria, and they shall lead to different optimal configurations. The reason lies in the fact that, unlike purely mechanical load, the thermal load is design-dependent and the two TO formulations lead to different load sensitivities. Another criterion based on the maximum von-Mises stress has also been adopted elsewhere, see [77].

2.2.4 Manufacturability-Related TO Problems

Apart from the performance-related constraints, the manufacturing limitations constitute another critical branch of design considerations. In the past years, relating work has mostly been driven by the constraints inherent in *subtractive* and *formative* manufacturing. Regarding the casting process, for instance, an additional linear constraint on artificial-density values of the elements in a column has been imposed in [79] and has later been implemented in the Altair OptiStruct. In the Ph.D thesis of Georgios Michailidis [78], three manufacturing constraints, including local thickness control, molding direction and thermal constraints, were dedicatedly treated. Two representative designs concerning molding constraint are herein provided in Fig. 5 for illustration purpose. One is recommended to refer to [22] for a complete review of similar methods.

2.2.5 Remarks

One should be aware that, according to different interests at stake, any of the constraints mentioned above are interchangeable with the objective function. Despite that some of these performance requirements are still not that mature to be applicable in engineering practice, some others have reached an industrial level of maturity in the last ten years. In what follows, successful applications of topology optimization in structural design are selectively presented.

2.3 Innovative Structural Design Issued from TO

Since the pioneering works [38, 39], successful applications of topology optimization are continuing to emerge, particularly in areas such as aerospace and aircraft, which are highly driven by the weight and cost savings. To illustrate the promising future of TO, we selectively present in this subsection several industrial structures innovated from TO, considering diverse performance requirements included in the previous subsection.

- *A380 Droop Nose Ribs light-weight design* The very first and the most popular application of TO was found in the design of a set of A380 Droop Nose Ribs. Figure 6 takes the A380 leading edge rib as an example to demonstrate the entire procedure. In collaboration with Altair Engineering, Airbus UK first found out initial designs for these Droop Nose Ribs via compliance-based TO, Fig. 6b. In the aim of providing more stability, these conceptual designs were subsequently engineered and were interpreted as a mixture of truss-design and shear-web design, as shown in Fig. 6c. Finally, by incorporating constraints such as stress, buckling, and manufacturing,

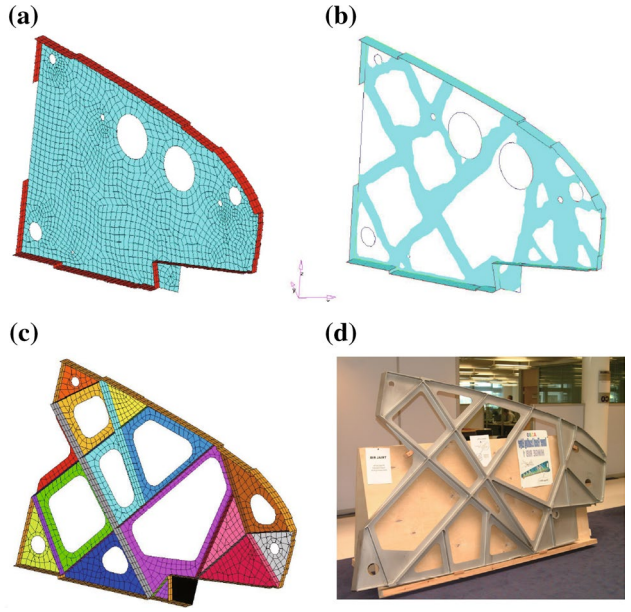

Fig. 6 Topology, size and shape optimization process for the design of aircraft component (A380 leading edge rib): **a** designable and non-designable region, **b** optimal design suggested by TO, **c** initial design for size and shape optimization and **d** a prototype machined from a high-strength aluminium alloy [80]

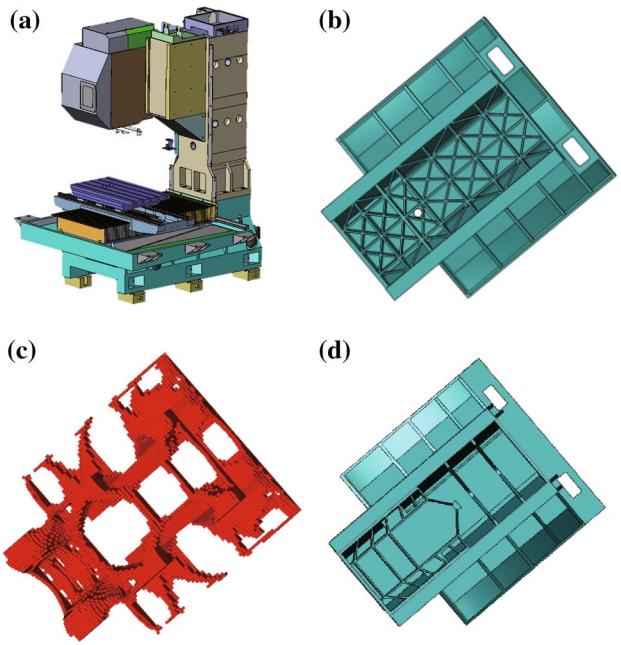

Fig. 7 Topology optimization performed on a high-precision machine tool to avoid non-uniform creep relaxation: **a** an illustrative example of a milling machine, **b** the initial design of the pedestal, **c** the configuration of the pedestal after topology optimization and **d** the final proposal after reconstruction [60]

a detailed size and shape optimization was performed for the final high-performance design. According to [80], a remarkable save of over 1000 kg has been achieved in total for the final designs, and other criteria including stress and local flange buckling were satisfied in the meantime. We underline that the success of the above optimization scheme relies on the good initial topologically optimized design. As pointed in [81], the major weight savings are achieved when selecting the type of design, but not when doing the detailed shape and size optimization.

- *Machine tool design for uniform reaction force distribution* Another successful example of TO lies in the design of the pedestal of a precision machine tool, Fig. 7. Responding to the need of avoiding non-uniform creep relaxation that deteriorates the levelness of the bench surface and the machining accuracy, a uniform distribution of vertical reaction forces over the pedestal supports was suggested to be beneficial [82, 83]. Given the importance of this matter in the long-term use of high- or ultra-precision machines, a topology optimization design procedure has been carried out, introducing *the variance of the reaction forces* as a quantitative description of this uniformity [60]. It turned out that the enhanced topology optimization model enabled a novel design of the pedestal, and a more even distribution of reaction forces was obtained over the six pedestal supports. Furthermore, the static/dynamic responses of the structure have also been improved, leading to a reduction of maximal displacement by 35% and a significant increase of the first several natural frequencies by around 15%.
- *Cockpit windshield shape-preserving design* We finally take the cockpit windshield design as the last example. Despite the damaging effects of bird strike and extreme weather condition, *warping deformation* around the cockpit windshield can be crucial to the windshield incidents. With this in consideration, [64] maintained the coordinate deformation of the windshield to avoid cracking by imposing local strain energies on specified shape preserving zones as additional design constraints. As illustrated in Fig. 8, the proposed shape preserving TO design distracts/redistributes critical loads that have led to large warping deformation. As a consequence, the strain energy measured on the elements around the windshield is reduced from 0.16 to 0.02 J. As pointed out in [9], this design criterion could also be suitable in the design of supporting structures with a large number of openings.

2.4 Remarks

We notice that the industrial application of TO can sometimes be cost-prohibitive in the sense of computing time for

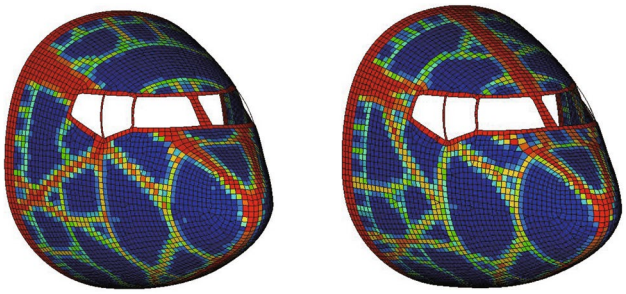

(a) Standard design **(b)** Shape-preserving design

Fig. 8 Airframe structures optimized with **a** standard TO method and **b** shape-preserving TO method, respectively. Structures such as stringers near rear fixations and roof structures probably distract critical loads that have led to large warping deformation [64]

large structures. To alleviate such issue, a technique combining parallel computing and domain decomposition has been developed in [84], and was proved to be applicable.

Furthermore, the designs obtained from topology optimization (Figs. 6, 7, 8), though of high performance, are difficult to be realized by conventional manufacturing processes such as subtractive machining and formative casting. Even if it is possible, the manufacturing can be too costly being aware that up to 98% of raw material—often of high quality and high value—can be machined away to produce the final part [85].

Fortunately, AM enables flexible production of complex parts while achieving at the same time a better buy-to-fly ratio.[4] This technique, preliminarily adopted for the rapid manufacturing of porous structures and prototypes [86, 87], is transforming in these days more and more from *rapid prototyping* to *rapid manufacturing*. The inherent benefits make it particularly appealing in the realization of topologically optimized structures. In this regard, the next section is devoted to the state-of-the-art of AM.

3 Recent Advances of 3D Printing

Additive Manufacturing, often termed Additive Layer Manufacturing (ALM), is defined, in the standard SS-EN ISO 52900: 2016, as *process of joining materials to make parts from 3D model data, usually layer upon layer, as opposed to subtractive and formative manufacturing methodologies* [88]. In this section, representative AM techniques and available commercial feedstocks are briefly presented to provide the readers with a panorama-size view. A group of dedicate

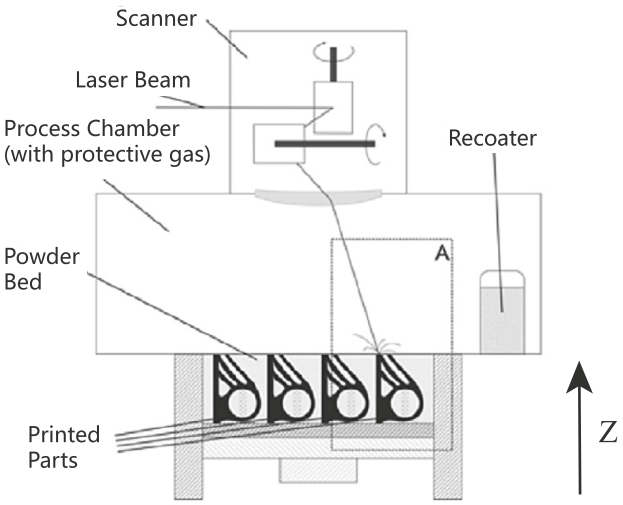

Fig. 9 Schematic of an LBM set up [87]

designs that have been realized using this innovative technology is also demonstrated.

3.1 The Panorama of Additive Manufacturing Techniques

AM processes, despite being diverse, basically share the same approach. We first load the 3D CAD model (in a .STL file) into a preparation software and generate some physical supports automatically to ensure a successful build. This model is then sliced together with the support, and an industry standard .SLC file is finally exported to the printer.

Proposed independently and to suit different interests, the nomenclatures of AM processes are, however, somewhat confusing. For example, the process of Laser Beam Melting (LBM) is also known as Selective Laser Melting (SLM) or Laser Metal Fusion (LMF), while Laser Metal Deposition (LMD) is the synonym of Direct Metal Deposition (DMD). For clarity, the following presentation of representative AM techniques shall revolve around two essential principles: (1) the nature and aggregate state of the feedstock and (2) the energy source of melting.

- *LBM* is a powder bed-based process, a typical system of which is illustrated in Fig. 9. Throughout the process, thin layers of atomized fine metal powder are evenly distributed using a coating mechanism (usually a leveling system or a recoating blade) onto the build plate that moves along the vertical (Z) axis. Once each layer is distributed, a high-power laser beam is directed in the X and Y directions to selectively expose the metal powder to the laser beam, according to the cross-section of the part. The build plate is then lowered after the selective exposure of the powder, and a new powder layer is applied

[4] The buy-to-fly ratio refers to the weight of the raw material purchased compared to the weight of the final part.

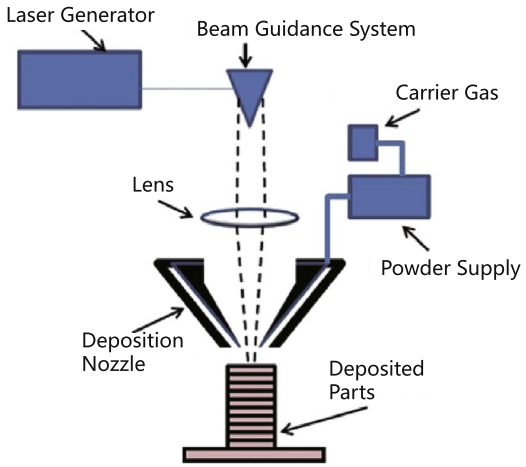

Fig. 10 Schematic of an LMD set up [91]

before repeating the process until the part is completed. Though the same process has also been referenced as Direct metal laser sintering (DMLS) in some research papers [89, 90], this naming can, however, be misleading since the laser energy is intense enough to *fully* melt each layer of metal powder, rather than just *sinter* it.

- *Electron beam melting (EBM)* Analogous to LBM, EBM is also a powder bed-based process. The most prominent difference between the two processes is that EBM uses an electron rather than a laser beam as the energy source to melt the metal powder. The electron beam, generated in an electron gun, is accelerated with an acceleration voltage and is finally directed to the desired position in the build plate (X–Y plane). A series of parameters such as beam current and speed function can be manipulated such that the power of the beam as well as the scan speed are controllable. Before printing each layer (distributed by a rake), the powder bed is generally first pre-heated by a defocused beam of high current and high speed in the aim of sintering the particles. Then, both the beam current and the scan speed are reduced during the subsequent melt scan to ensure the complete melting of the powder. The process of powder spreading, pre-scanning and scanning, and build plate lowering is repeated until the part is finished.
- *Laser metal deposition (LMD)* Laser metal deposition (LMD), also called laser deposition welding, is another generative laser procedure that is quite different from the powder bed-based ones (Fig. 10). In this process, metal is applied to *existing* tools and components in layers. This technology has long been practiced for coating and to repair high-value parts by systematically refining or combining materials. In contrast to SLM, LMD generates first a weld pool into which metal powder is automatically fed with a coaxial or multi-jet nozzle [91]. The powder then melts to form a deposit that is fusion-bonded to the substrate. After depositing each layer, the part remains stationary in most commonly seen LMD systems, and the laser, as well as the nozzle is manipulated by a gantry system or a robotic arm to continue the process. This difference to LBM enables by consequence a comparatively large build volume in LMD systems. Besides, the high build-up rate and therefore the fast process speed are two other advantages of LMD over LBM technique. Over the years, extensive research work has led to a range of similar systems, in which either the part is repositioned under a stationary deposition head, or wires are adopted as feedstocks, instead of using nozzles and metal powders [92].

In previous paragraphs, we have been focusing on the most popular *metallic* AM techniques that allow the production of critical parts in engineering practice. It is however noted that there also exist other AM systems developed on the basis of diverse non-metal materials. The molten plastic, among others, is the most popular one. Stereolithography (SLA), for example, builds each layer by focusing an ultraviolet (UV) laser onto a vat of photopolymer resin [93]. The photopolymer, liquid at its original state, is photochemically solidified after the exposure to ultraviolet light. Other systems that work on bio- or ceramic- materials go however beyond the scope of the current work, and readers are referred to [94–96] and the references therein.

3.2 Feedstock for AM

It has become nowadays possible to reliably manufacture dense parts with outstanding properties in the use of diverse materials, including, among others, steel, aluminium, and titanium.

3.2.1 Steel

Steel is of high interest for AM systems since it is considered as the most common material till date, and its alloys satisfy typical requirements of general-purpose applications [97]. Austenitic stainless steels, maraging steel, as well as precipitation hardenable stainless steels were reported to be available mainly for LBM [98–100], while tool steels, in contrast, have been mainly used for EBM [101].

3.2.2 Titanium

Titanium is chosen based around its particular appeal to the aerospace industry. Given the low weight, high specific strength, high creep strength at high temperature and corrosion resistance [102], Ti and Ti alloys have been extensively employed to produce such high-performance parts as

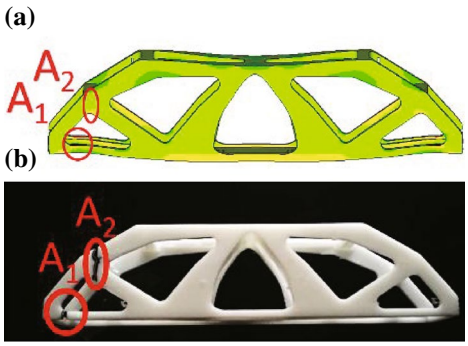

Fig. 11 An example of SLA in verifying the topologically optimized MBB beam: A_1 and A_2 indicate locations where stress concentrations are observed [107]

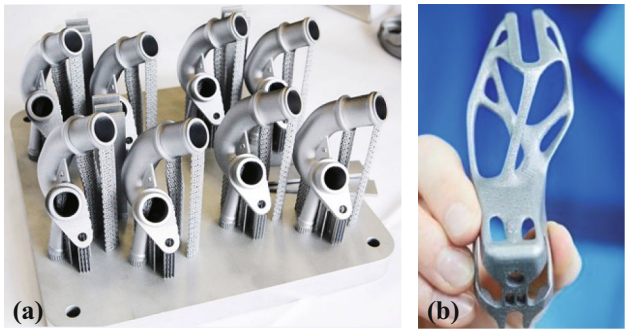

Fig. 12 Examples of AM parts in the automotive industry: **a** reproductions on demand of water connectors for the Audi W12 engine and **b** the fixture in the tonneau cover for the soft-top of i8 Roadster [115, 116]

rotating components in turbine engines. Universally applicable to LBM, EBM [103] and LMD [104], Ti–6Al–4V has hitherto been widely adopted for commercial fabrication. Besides, given the variety of alloy compositions and related microstructures, Ti-based alloys have also drawn the most significant interest of research in investigating the relationship between different AM processes and the resulting microstructures as well as the printed properties [105].

3.2.3 Aluminium

Aluminium and its alloys are adopted, however, in a rather limited manner in AM. The factors to cause this less-common usage are (1) lack of weldability and (2) lower commercial interest in AM due to their good and easy processability via conventional manufacutring techniques [106]. Taking the high-performance alloy EN AW-7075 as an example, the presence of highly volatile elements such as Zn leads easily to the turbulent melt pools, splatters and porosities during the forming process, thus is not suited for AM. Up till today, the combination of LBM and Alsi10 Mg has dominated the aluminium parts formed by AM [87].

In spite of metal powder, polymeric composite and molten plastic such as photo-polymers constitute another branch of AM feedstock [108, 109]. With its relative low-cost and easy accessibility, the adoption of resin has made AM technologies much more affordable. During the past years, many laboratories specialized in TO have employed this technique to print the topologically optimized designs in the purpose of validating their mechanical performances. One can find such an example in Fig. 11, where the failure mode of the optimal design has been validated on a printed specimen. Ceramics and organic materials, interesting in specific disciplines, are out of the scope of the current work. That said, the material diversity allows a high number of properties to be embedded into the final products, and we are witnessing a steady progress that expands the portfolio of available materials.

3.3 Industrialization of AM

Over the last few years, AM has taken a considerable step towards the industrialization and is progressing rapidly [88]. This generalization, started with dental and medical implants and then followed by aeronautic parts, is covering more and more fields where full series and multi-functional products have been in place. In what follows, we cite a group of successful applications in the automotive and aerospace sectors, where AM has found the highest degree of acceptance and implementation.

3.3.1 Automotive

In the automotive sector, the AM technique has long been and continues to be a source of product innovation thanks to its extremely high flexibility. BMW, for example, is now producing each year over 25,000 prototype parts which have sped up the design phase significantly [110]. Ford, similarly, has skipped the need for tooling by creating prototypes using AM and saved millions of dollars in product development costs [111, 112]. However, we need to be aware that the associated high cost and slow print speed have hindered AM from being used for mass production, at least thus far.

The opportunity has encouraged more and more technology advances, and global automakers are currently moving from AM sheerly for prototyping purpose to making parts that go right into the vehicles. For instance, the gearstick for the Porsche 959, the water connector for the Audi W12 engine and the fixture in the tonneau cover for the soft-top of i8 Roadster have all been additively manufactured in this day (Fig. 12). A research project is also underway at the Volkswagen Osnabruck to reinforce an A-pillar using metallic AM. Furthermore, Ford has been working with the

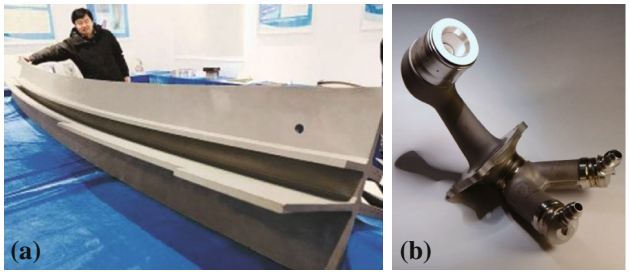

Fig. 13 Examples of AM parts in the aerospace industry: **a** central wing spar for Comac C919 passenger-plane and **b** fuel nozzle for GE's LEAP 1-A engine [120, 121]

Carbon 3D to produce automotive parts from UV curable resins since 2014 [113]. As a consequence, the original replacement parts no longer held in warehouses can henceforth be reproduced on-site, and maintenance and repair will be accelerated significantly [114] has outlined four tactical adoption paths and concluded the extent to which the potential can be offered by AM. Given the current circumstances, we firmly believe that AM will be a driver of supply chain transformation, and we are also convinced that this innovative technique will be more and more used in the automotive sector.

3.3.2 Aerospace

Due to the presence of components featuring complex geometries that are difficult to be manufactured conventionally, the aerospace is another field which has been radically affected by AM. Prominent examples include Airbus A320 nacelle hinge bracket, bracket for high lift device and high-value aerospace bracket [85, 117–119]. More recently, the State Key Laboratory of Solidification Processing, Northwestern Polytechnical University (NPU), China, has additively manufactured a central wing spar of 5 m long, Fig. 13a, for the Comac C919 passenger-plane, which has entered commercial service in 2016. The mechanical properties of the printed spar were said to meet the standard of forged parts.

In addition to its great potential in producing complex parts, AM enables in the meantime *the reduction of the number of individual parts* in the component, and by consequence, the cost related to the assembly followed up. Taking the manufacturing of an automotive A-pillar as an example, it was reported that the reduction of individual parts could be as high as over 74%, significantly reducing the total weight without negatively impacting its durability. Another example lies in the manufacturing of a fuel nozzle for the GE's LEAP-1 engine, Fig. 13b, in which AM printed all 20 parts of the nozzle into a single unit that weighted 25% less and was five times more durable than its predecessors.

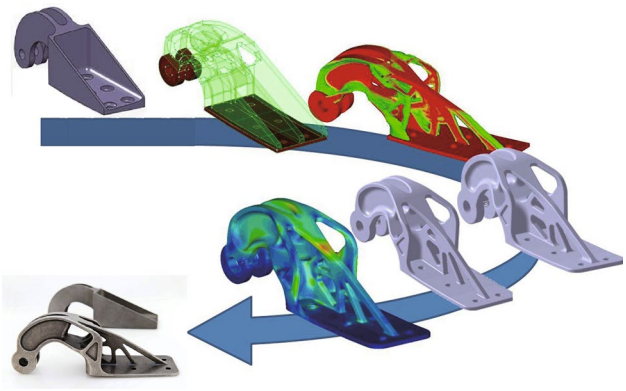

Fig. 14 Airbus A320 Nacelle Hinge Bracket redesigned for additive manufacturing through topology optimization [117]

In summary, we conclude that companies in the automotive and the aerospace industries have embraced the paradigm shift towards DfAM, and others are following suit [122]. It is also anticipated that this cutting-edge technique would surely be a game changer in the near future.

3.4 An Ideal "Marriage" Between AM and TO

Successful applications have fully displayed the core competence of AM in fabricating dedicate structural designs in Sect. 3.3. Considering the difficulties in bringing TO-based designs into reality with conventional manufacturing methodologies, one naturally agrees to the idea of employing AM for their realizations. Considerable success has been reported regarding this combination since then, and we provide hereby several representative examples.

The EOS and the Airbus Group Innovations of Filton, Bristol, have since 2014 carried out a joint study on an Airbus A320 nacelle hinge bracket (Fig. 14). It was demonstrated in this study that, compared with conventional casting process used as the baseline, Direct Metal Laser Sintering (DMLS) has the advantage of integrating business and ecological sustainability. Specifically speaking, the manufacturing freedom offered by the AM process allowed a topologically optimized design to be readily realized and as a consequence, the CO_2 emission over the whole lifecycle of the nacelle hinges was reduced by nearly 40% via weight reduction. Furthermore, by eliminating waste from secondary machining, a noteworthy saving of weight from 918 (steel) to 326 g (titanium) was also observed through two loops of optimization, although the change in material accounts for roughly half of this change in mass. As pointed out in the final report of Jon Meyer, Additive Layer Manufacturing Research Team Leader, "*DMLS has demonstrated a number of benefits, as it can support the optimization of design and enable subsequent manufacture in low-volume production*" [124].

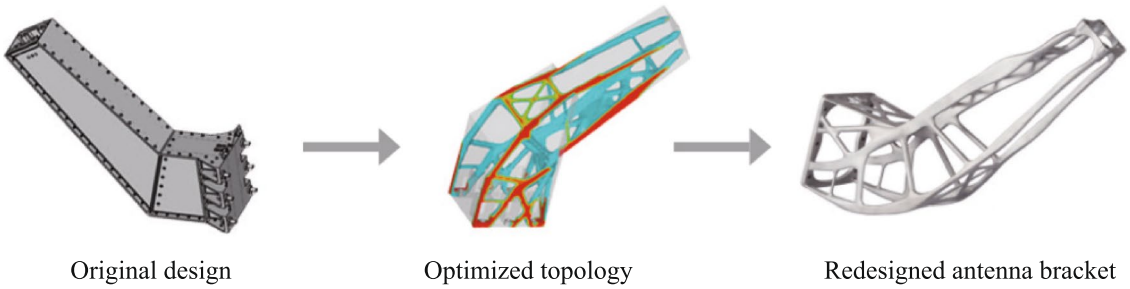

Fig. 15 The technological symbiosis of TO and AM results in a halving in weight, reduced stress, increased stiffness and a minimum of design lead time [123]

We further emphasise that this technological symbiosis is also observed even beyond the Earth's atmosphere. We adopt here the RUAG'S Sentinel satellite as an example. Figure 15 demonstrates an entire topology optimization procedure of the antenna bracket for additive manufacturing. In this said work, the design optimization was driven by two essentials: (1) the requirement in shaving excess weight and (2) the minimization of undesired vibration issued from the very high speed (up to several 1000 km per hour during a rocket launch). The optimal design was finally printed with aluminium alloyed AlSi10Mg, which was characterized by its high strength and strong resistance to dynamic stress. The result of such efforts was a significant reduction in the weight of the final component: down to 0.94 kg from 1.6 kg, representing a saving of over 40% [123]. The component characteristics have proved their worth in tests carried out with the requisite stringency for the aerospace sector. The new design, exceeding all its predecessors, was certified for deployment in outer space.

4 From Design to Manufacturing to Product Use: An Illustrative Example

In this section, a complete procedure of DfAM is carried out taking an aerospace bracket as an example. The primary interest of optimizing such structure, outlined by Kranz et al. [125], lies in the significant optimization-induced weight saving given the extensive use of similar parts in the assembly of an aircraft. Through a careful verification on the original design proposal of the bracket (Fig. 16), we noticed that all mechanical performances were satisfied with a safety factor of over 2.5, providing a considerably large margin for further light-weight design. In what follows, the bracket is designed by employing the topology optimization technique, which is then followed by a size optimization procedure. The optimal design is finally realized by additive manufacturing of titanium alloy powder, and a performance verification is carried out to ensure the product use.

4.1 Problem Description

Since the part acts as a connector between the fuselage and the aero-engine, a concentrated force F_x is equivalently applied to include the thrust load from the engine. In numerical modeling, this force is imposed at the keypoint KP, which is connected to the suspension hole with a group of MPC (i.e., multi-point constraint) elements. Besides, an inertia force, decomposed into a transverse F_y and a vertical F_z component, is applied at the same location. For reasons of confidentiality, the values of these loads are normalized in such a way that their corresponding amplitudes are proportional to the lengths of vectors as illustrated in Fig. 16. Moreover, because of the temperature gradient between the engine and the fuselage, we consider also a thermal load to be applied on the part, and a coupled thermo-elastic problem needs to be solved

$$\mathbf{KU} = \mathbf{F^a} + \mathbf{F^{th}}, \tag{4}$$

in which $\mathbf{K}$ is the global stiffness matrix and $\mathbf{U}$ the nodal displacement vector. $\mathbf{F^a}$ and $\mathbf{F^{th}}$ correspond to the equivalent

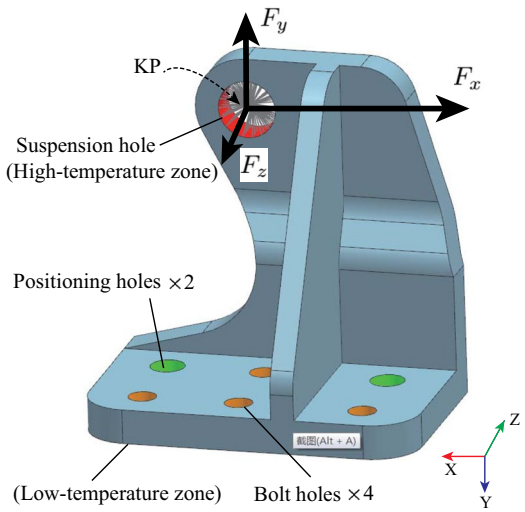

Fig. 16 Current design of the aerospace bracket

force and thermal load vectors, respectively. Note that, at the finite element level, the nodal vector of thermal stress is expressed as

$$\mathbf{F}_\mathbf{e}^{\mathbf{th}} = \beta_e \overline{\mathbf{F}_\mathbf{e}^{\mathbf{th}}}, \tag{5}$$

where β_e, the thermal stress coefficient, is related to the Young's modulus (E), the thermal expansion coefficient (α) and the Poisson's ratio (μ) with $\beta_e = E_e\alpha_e/(1-2\mu_e)$, and

$$\overline{\mathbf{F}_\mathbf{e}^{\mathbf{th}}} = \int_{\Omega_e} \mathbf{B}_\mathbf{e}^{\mathbf{T}} \boldsymbol{\phi} \Delta T_e d\Omega. \tag{6}$$

Here ΔT_e denotes the elemental temperature rise, and $\boldsymbol{\phi} = [1 \quad 1 \quad 1 \quad 0 \quad 0 \quad 0]$ for this 3D case.

4.2 Thermo-Elastic Topology Optimization

In solving the current thermo-elastic topology optimization problem, we seek to minimize the global compliance of the bracket under the load conditions previously described in Sect. 4.1. In spite of a volume fraction set at 0.15, another constraint is imposed on the horizontal displacement measured on the specified key point KP, i.e., u_x^{KP}. A threshold value of 0.5 mm was proposed referring to that of the initial design. The formulation of this optimization problem is expressed as

$$\begin{aligned} \arg\min_{\rho} \quad & C = \mathbf{U}^{\mathbf{T}}\mathbf{K}(\boldsymbol{\rho})\mathbf{U}, \quad \boldsymbol{\rho} = \left(\rho_1, \rho_2 \cdots \rho_N\right) \\ s.t. \quad & K(\boldsymbol{\rho})\mathbf{U} = \mathbf{F}^{\mathbf{a}} + \mathbf{F}^{\mathbf{th}}(\boldsymbol{\rho}) \\ & \mathbf{H}(\boldsymbol{\rho})\mathbf{T} = \mathbf{P} \\ & V \le 0.15V^0 \\ & u_x^{\mathrm{KP}} \le 0.5 \\ & 0 < \rho_i \le 1, \quad i = 1, 2 \ldots N \end{aligned} \tag{7}$$

in which $\mathbf{H}$ is the heat conductivity matrix and $\mathbf{T}$ denotes the temperature field. We emphasise that, unlike the applied mechanical force $\mathbf{F}^{\mathbf{a}}$ and the thermal load $\mathbf{P}$ which are design-independent, the thermal stress load vector $\mathbf{F}^{\mathbf{th}}$ distinctly depends on the design variables.

The design domain is defined as a cuboid enveloping the initial design, and the bottom surface of the bracket (low-temperature zone) and the four bolt holes (orange surfaces in Fig. 16) are constrained along Y-axis. The two positioning holes (green surfaces) are fixed. From an engineering perspective and inspired from the original design, areas around the four fastener holes and the two positioning holes are treated as non-designable regions, Fig. 17b. By solving the problem in Eq. (7), the optimized structural configuration of the aerospace bracket is presented in Fig. 18a. The stress

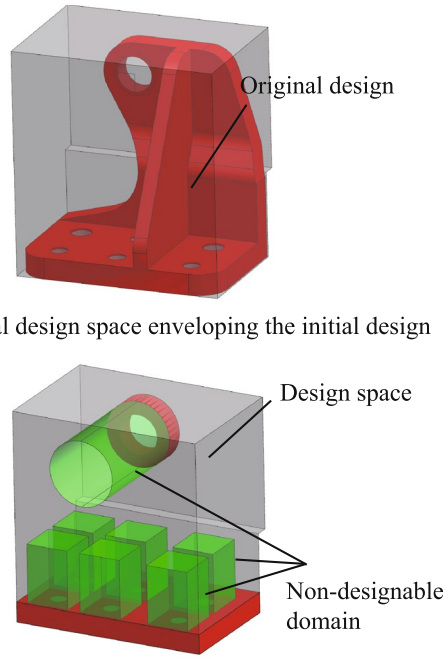

(a) Total design space enveloping the initial design

(b) Design domain with non-designable areas

Fig. 17 Geometric model for topology optimization

constraint, not included in the topology optimization, is considered later at the phase of size optimization.

4.3 Reconstruction and Size Optimization

From the topologically optimized design in Fig. 18a, a reconstruction model is built with engineering expertise by researchers from Beijing Aerospace Technology Institute, China. A size optimization procedure is further carried out to achieve the final design of the bracket while validating other performance requirements such as allowable stress. We choose at this stage the structural mass as the objective of the size optimization problem such that the final design remains weight-competitive. The thicknesses of 10 critical zones are considered as design variables. As for the performance constraints, other than the restricted horizontal displacement on KP, a maximum von-Mises stress level of 650 MPa is additionally imposed, and the buckling factor is desired to be no less than 60.

We propose an increment of ± 0.5 mm for all design variables during iterations, and the final design after size optimization is observed in Fig. 18b. For comparison reasons, we list in Table 1 the objective function and the constraint values before and after optimization, with that of the original design used as the baseline. As observed, the mass of the aerospace bracket is reduced by 18.3%, benefiting from topology and size

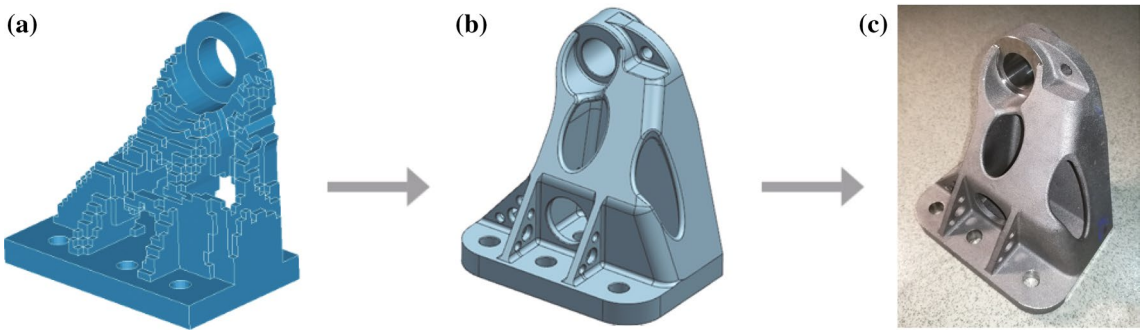

Fig. 18 **a** Topology optimal design of the bracket, **b** Reconstructed design for size optimization and **c** final design realized by LBM

Table 1 Comparison of the objective and constraints before and after optimization

	Mass (kg)	u_x^{KP} (mm)	Max. von-Mises stress (MPa)	Buckling factor
Original design	1.91	0.47	554.8	46.7
Final optimal design	1.56	0.4	636.4	59.6

optimization, and the three constraints are satisfied as well in the final design.

4.4 Additive Manufacturing of the Aerospace Bracket

By using the BLT-S300 platform from Xi'an Bright Laser Technologies Co., Ltd (BLT),[5] the optimal design of the aircraft bracket was additively manufactured with the LBM technique. The raw material used is the titanium-alloy TC4. The precursor powder's particle size is rather fine, ranging from 15 to 53 µm. Note that, after printing each layer, the scanning trajectory is rotated for 67°. Besides, other processing parameters such as laser power of 360 W, layer thickness of 60 µm and hatching space of 120 µm, have all been carefully chosen by experimentalist from BLT to guarantee a good performance of the printed part. Furthermore, to reduce the amount of support and to ensure their easy removal, the CAD model has also been rotated about 20° along the X-axis before preparing the slicing model. The final printed bracket is presented in Fig. 18c.

4.5 Experimental Validation

To examine the material properties of the final part, we printed a group of three dog-bone specimens simultaneously with the bracket. By carrying out tensile tests on these standard specimens, we derived an averaged Young's modulus of 110 GPa and a Poisson's ratio of 0.34. The tensile strength and the 0.2% yield strength were observed to equal to 1275 and 1140 MPa, respectively. By comparing with the metal powder properties provided by the supplier, these obtained properties are entirely satisfactory and the processing parameters are affirmed.

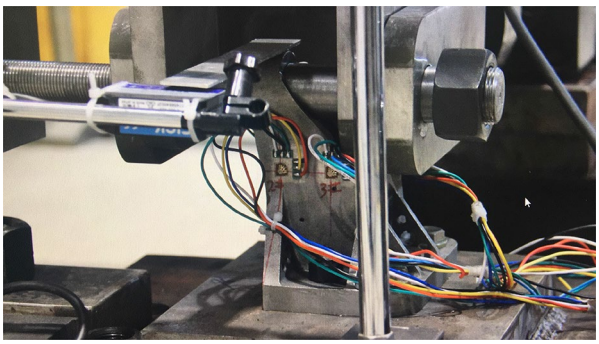

Fig. 19 Experimental setting for the tri-axial tensile test

Given the extreme loading condition of the part in service, we further conduct a tri-axial tensile test, and the experimental setting is provided in Fig. 19. The horizontal displacement at KP is recorded while loading, and a value of 0.61 mm is attained at the maximum load. Please note that this value, despite violating the displacement constraint in Eq. (7), is still considered acceptable in view of the possible experimental error. Taking into account also the comparatively large safety factor, the optimal design is certified for product use.

[5] BLT is one of China's largest manufacturers of metal additive manufacturing systems.

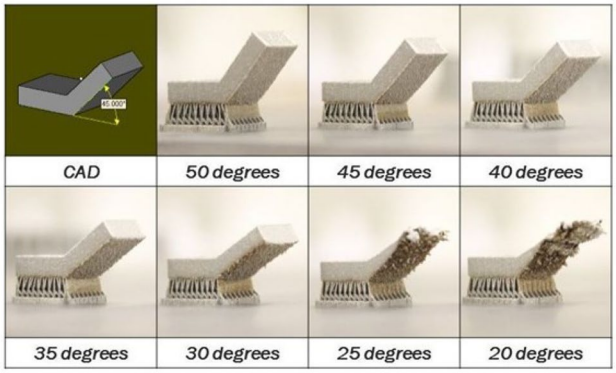

Fig. 20 Overhang tests showing different printabilities and finish qualities at seven different angles [126]

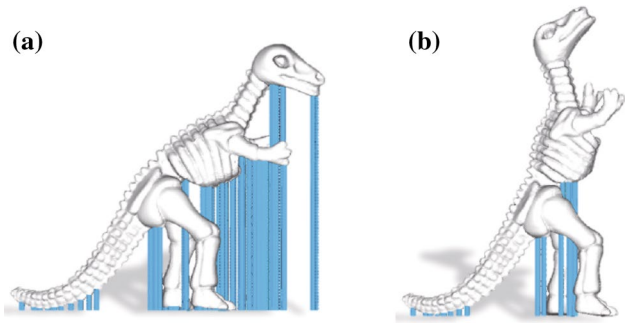

Fig. 21 An orientation-driven shape optimization procedure that leads to significant reduction of material usage for slimming support: **a** the initial design and **b** the adjusted new proposal with the support indicated in blue [127]

5 On Challenges and Strategies in Fabricating Critical High-Performance Parts via TO and 3D Printing

Despite the promising results reported in relating to AM, one must be aware of the potential underperformance of the technology. Since about 10 years, engineering practice has fully exposed a number of limitations of AM concerning both the *geometrical accuracy* and the *service performance* of the printed part. For example, analogous to any other conventional manufacturing technique, AM does present certain manufacturability-related constraints, which could easily lead to the failure of the print if not properly considered. Moreover, due to the layer-by-layer printing manner and the microscale-control characteristics, the mechanical properties of the printed part may present undesired porosity and anisotropy that are crucial to the structural performance. These issues, still under investigation, need to be carefully addressed to promote a long-term partnership between TO and AM.

5.1 Loss of Geometric Accuracy: Overhang Feature and Staircase Effect

The first issue which has drawn the attention of researchers appeared in printing large overhang features. As illustrated in Fig. 20, parts are printed with a bottom-up approach, and those with overhang angles of 50°, 45° and 40° are readily printed without any support while still obtaining smooth overhang surfaces. However, the chance of such successful build drops as the angle of the unsupported feature decreases. At the angle of 25°, for instance, a rough and unfinished-looking surface is obtained.

A simple remedy to this issue is to print some support structures along with the work-piece. Unfortunately, this measure is at the price of slowing down the process and entails inevitably post-processing. Besides, the removal of such sacrificial features can be onerous as the complexity of the component increases. Furthermore, the remaining support structures or the small defects induced by their removal may affect the quality of the final part in an undesired manner. For these reasons, the overhang features need to be considered beforehand to obtain a print-friendly design. Up till today, extensive efforts have been devoted in this endeavour, and the many directions explored are classified into the following categories:

1. Slimming support design;
2. Optimal build direction design;
3. Non-vertical support design;
4. Self-support design.

In the first place, the most straightforward solution to overhang features lies in the posterior introduction of supplementary material to the optimal design, which however violates the mass constraint. Demands have therefore been placed on the slimming down of support structures. For this purpose, an extra constraint on the quantity of material used in the support structure was suggested and was incorporated within the design frame. By slightly adjusting the "facing-down" surface facets, Hu et al. [127] proposed an orientation-driven shape optimization approach to minimize the support volume. In the aim of guaranteeing a minimum change in the design, the said work adopted the energy of rigidity, defined on a volumetric mesh enclosing the original design, as the objective function. As observed from Fig. 21, the usage of scaffold structures has been largely cut down, representing a reduction of over 70% through optimization. It is however pertinent to point out that this technique applies mainly to such applications where the model can be adjusted before finalizing the design.

To avoid modifying the final design, another alternative seeks to optimize the building direction such that a minimum material usage shall be entailed. To this end, the three

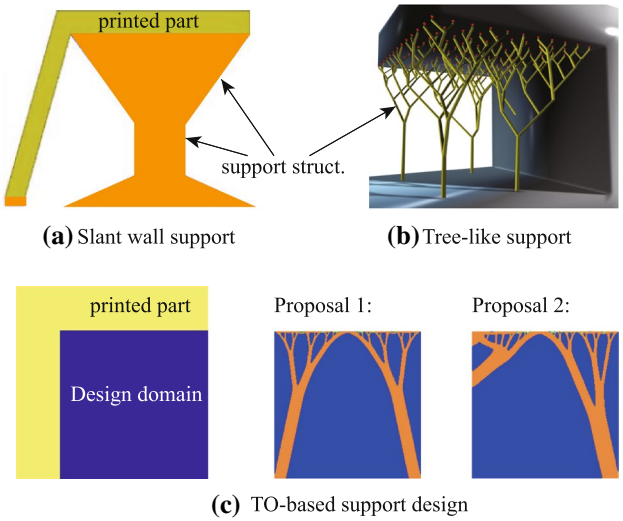

Fig. 22 Examples of non-vertical slimming supports [131–133]

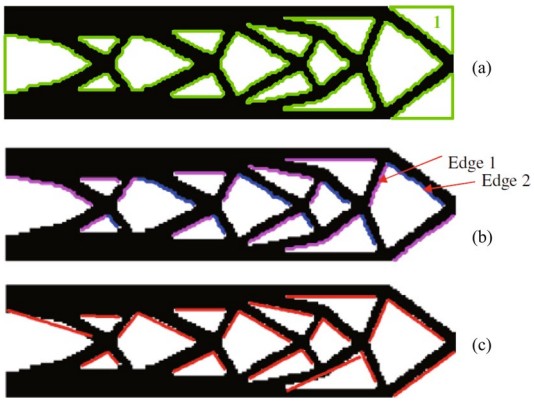

Fig. 23 An edge analysis procedure to design self-support structures: **a** identification of cavities boundaries, **b** identification of downward facing edges and **c** straight line approximated edges to calculate overhang angles [136]

components of the normal vector of the base plate were generally considered as design variables, and the objective function, i.e., the support volume, was calculated on top of the minimum printable angle. Despite the rotation of the base plate around Z-axis being independent of the support volume, the transformation matrix is provided, in the interests of consistency, with three rotation angles α, β and γ with respect to X, Y and Z axis

$$\mathbf{R} = \begin{pmatrix} 1 & 0 & 0 \\ 0 & \cos\alpha & -\sin\alpha \\ 0 & \sin\alpha & \cos\alpha \end{pmatrix} \begin{pmatrix} \cos\beta & 0 & \sin\beta \\ 0 & 1 & 0 \\ -\sin\beta & 0 & \cos\beta \end{pmatrix} \begin{pmatrix} \cos\gamma & -\sin\gamma & 0 \\ \sin\gamma & \cos\gamma & 0 \\ 0 & 0 & 1 \end{pmatrix}. \tag{8}$$

A prime example of such method has been presented in [128], where the support material volume was approximated by the irregular triangular prism formed when the triangle was projected onto the base plate. The optimization procedure, having been tested on different geometries of increasing complexity, was shown to bring a general improvement over orientations recommended by preprocessing softwares. Despite that, the authors suggested that the method be incorporated with the expertise of the manufacturers. Additionally, considering the impact of orientation on the building height, and by consequence the build time required, research effort has also been devoted to solving a multi-objective optimization problem in which both the build time and the support material volume are minimized. Readers are referred to [129, 130] for more details.

Other than adopting support structures that are perpendicular to the build plate, another group of methods consists in designing non-vertical supports (Fig. 22). These methods were proved to be practical since they take full advantage of the printability of sloping features. Pioneering work suggested the adoption of slant wall support [131], the slope of which is designed to be no smaller than the critical overhang angle. Experimental results showed that these supports assist well the fabrication of parts while reducing the material usage by averagely 30%. Later, other more advanced non-vertical supports such as tree-like structure [132] and bridge-like scaffolds [134] have also been proposed, and a more considerable saving of support material was attained, amounting even to 70%. These non-vertical support design techniques, albeit heuristic, can now be automatically implemented and place no demands on the operator's experience [135]. More recently, Mezzadri et al. [133] has formulated the generation of support structures for AM as a novel TO problem. The support design in such case is rich in mechanical meaning, that is, the support structure needs to be stiff enough to support the material above. This method enables the design of support not limited only to those grown from the build plate, but also from the already printed regions. An illustrative example is provided in Fig. 22c.

In these days, other than the strategies mentioned above, the community of TO has also paid great attention to design support-free structures, and fruitful results have been reported. Notably, Bracke et al. [136] carried out an edge analysis and quantified the overall violation of self-support requirements as a penalty function, which was then incorporated into the objective function through the use of a weighting parameter (Fig. 23). However, the sensitivity analysis related to the suggested constraint has created bottlenecks and delays in its implementation. More recently, Zhang and Zhou [137] explicitly included the overhang constraints under the framework of Feature-driven Optimization (FDO) by employing polygon features as design primitives (Fig. 24). The advantage of such method lies in

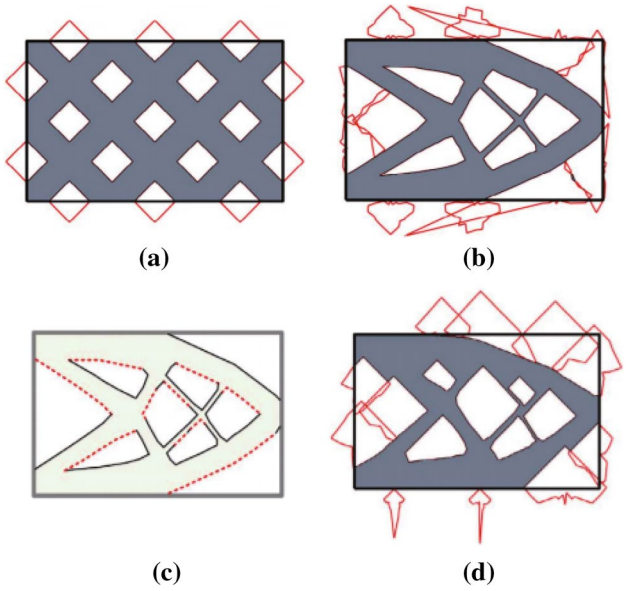

Fig. 24 **a** The cantilever beam to be optimized (with the 17 designable polygons distributed within the design domain), **b** the configuration of free-form optimal design, **c** boundaries requiring support identified with a printable overhang angle of 45° and **d** the final optimized self-support design [137]

the simplicity of the expression of constraints as inclined angles readily obtained from the design boundaries.

It is noteworthy that, despite seeing rapid development, these methodologies are still in their infancy and have been tested mainly for 2D cases, and on the basis of the "Rule of thumb" for printable overhang angle. Since the threshold value of printable overhang angle was reported to be dependent on the printing orientation, continuing efforts are still needed for 3D cases. In the meantime, we have to admit that the use of support structures is twofold. Despite the tedious and time-consuming support design and removal, it should not be forgotten that the support structures are sometimes subjectively generated to dissipate process heat into the building platform to avoid local distortion of parts [128].

Aside from the unprintable large overhang areas, we note also that the dimensional accuracy and finish quality of printed parts are not satisfactory and always lead to the so-called "*staircase effect*". This characteristics of AM parts has been mostly restricted by the printing apparatus in use, particularly the spot size diameter. According to [138], in metallic AM, we generally obtain a surface finish of the order of 10–100 µm, which, unfortunately, is not in the range of high-precision. Though AM techniques such as EBM promise to significantly enhance the surface finish [139], the staircase effect is still a salient issue for high-performance components. Past experience has revealed that it can be reduced by carefully choosing the process parameters (say, for example, the hatch distance). The so-called hybrid

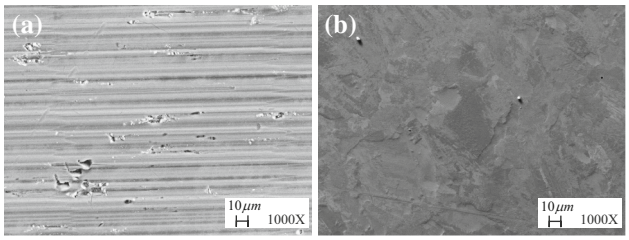

Fig. 25 SEM images of the as-printed specimens prepared: **a** perpendicular to the build plate and **b** parallel to the build plate

manufacturing, on the other hand, has also been employed in engineering practice by combining AM with other conventional manufacturing methodologies such as milling and forging. One can find such an example in [114], where the authors have taken full advantage of AM in printing features such as lattice structures, while still ensuring a uniform finish quality with the aid of CNC milling. Such a hybrid additive/subtractive system has come to reality in SonicLayer 4000 [140].

5.2 Performance Deterioration: Low Repeatability, Residual Stress, and Anisotropy

Other than the inability of printing specific geometries and the resulting low finish quality, AM parts are, in most cases, plagued with a certain performance deterioration. Given the presence of undesired and locally-distributed porosities (Fig. 25), it is a widely accepted fact that AM formed parts suffer from relatively low repeatability, which is among the leading causes that have hindered its application in mass production. This low repeatability, on a deeper level, is attributed to the micro- to macro-scale process control and the unique metallurgical phenomena stemmed from the non-equilibrium physical and chemical nature during printing [141]. The resulting defects throughout the part were reported to lead notably to a reduction of strength and fatigue life, given that the fracture is generally initiated at large surface void [142].

On the other hand, since the previously solidified layers are re-melted and cooled several times at inconsistent levels of heat, severe residual stresses (RS) can arise during the process such as LBM. This heat-cycling induced RS, leading not only to the loss of geometric accuracy beyond tolerance, may also result in cracking or even cause failure of printing in certain extreme cases (Fig. 26).

Analogous to the low repeatability, the printed parts were also reported to experience significant anisotropy. Under the framework of metallic AM, this anisotropy was issued from the directional solidification and the rapid cooling rate associated with the AM process. More specifically, it was explained by the epitaxially grown microstructures [87].

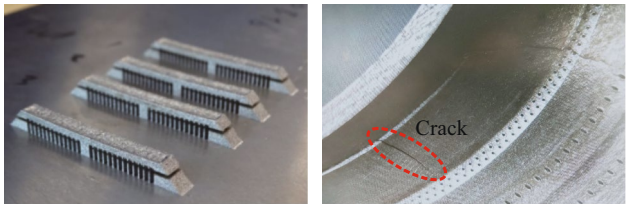

(a) Beam deflection **(b)** Cracking initiation

Fig. 26 **a** Beam deflection arising upon support cutting and **b** crack initiated from residual stress observed on the as-printed part ([143] and BLT)

However, the factors determining the extent to which the anisotropy would be manifested are various, including, in addition to the printing techniques, the adopted parameter settings and raw material in use. It seems therefore understandable that entirely different results have been reported concerning the printed anisotropy. For instance, some claimed that the as-deposited samples exhibit higher strength and lower ductility for the longitudinal direction than for the transverse direction [144–146], while some others have observed by contrast a good consistency of maximum strength for a group of LBM fabricated dog-bone specimens obtained with varying printing direction [147, 148]. Moreover, concerning the SLA printed part, a characteristics of transverse isotropy with anisotropy along the building direction has been reported in [107]. In any case, the understanding of such anisotropy could have a non-negligible impact on the part performance. Figure 27 demonstrates that a better structural performance is achieved if taking into account the anisotropy of the printed parts at the design stage, in comparison with conventional models where material properties were considered isotropic.

In the purpose of thoroughly understanding these process-related limitations, and hence bringing about the elimination thereof, extensive research has been carried out along with different directions. Through a survey of the literature, we have identified two primary study interests focusing on:

- *Process modelling* In the aim of yielding good consistency and better mechanical properties, the optimization of processing parameters was always necessitated. Many numerical models have been developed in this endeavour, and they were categorized mainly into two groups: the general process models [149–151] and those characterizing specific aspects of the process, such as heat transfer, stress distribution, and material phase change [152–155]. Various part- and machine-specific examples have proved that these models are reliable in predicting the temperature and stress fields during the print, and in driving the optimization of process parameters [143, 156, 157]. However, it is an undeniable fact that these models can be very cumbersome to use for general problems, and experiments need to be carefully designed to tune and verify the numerical model in real time. Discussed in detail in [158], the pros and cons of these models need no further elaboration.

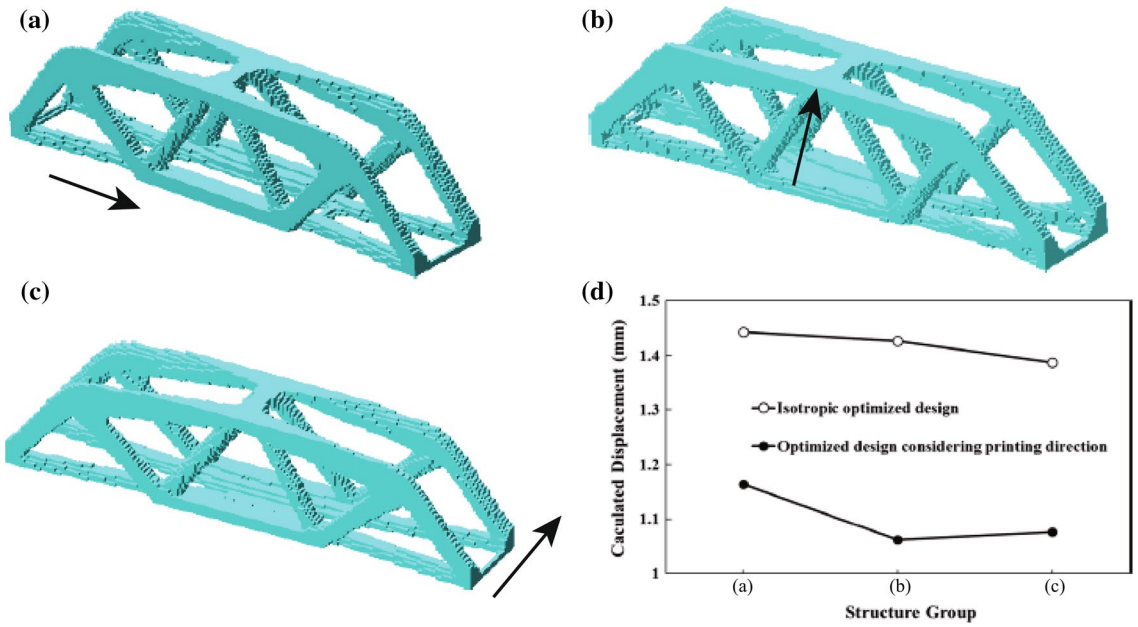

Fig. 27 **a–c** Topology optimization designs considering directional transversely isotropic with the printing direction indicated by the arrow and **d** stiffness improvement comparing with isotropic optimized design [107]

- *Process control and post-processing* It was reported that process control and post-processing were the most common and straightforward practices to mitigate the above-mentioned inconvenient situations [159, 160]. Up till today, the length and orientation of the laser scan vectors, island scanning, overlap rates, and hatch angles, among others, have all been reported in this regard [161]. For example, Wu et al. [36] successfully reduced the RS measured on the as-printed part by decreasing scan island size, or by increasing the applied energy per unit length (laser power/speed). The influence of thermal process such as post-curing, heating the powder bed during printing and pre- or re-scanning each layer before printing has also been carefully investigated. It is now a well-documented fact that the thermal process may alleviate the insufficient melting phenomenon, and significantly improve the mechanical properties, the residual stress in particular [162].

It is however worthy to note that the above quality control measures depend usually on a deep insight into the mechanism of microstructure evolution during the printing process. Growing demand has thus been placed on the evaluation of the part's physical properties and RS levels in the microscopic level, and on their correlation with various processing parameters. The optical as well as mechanical process monitoring, despite being both time-consuming and less cost-effective, seems to be unavoidable. A brief literature review shows that metallographic and crystallographic characterization techniques such as Optical Microscope (OM), Scanning Electron Microscope (SEM), X-ray diffraction and Electron backscatter diffraction (EBSD) were extensively used [87, 141, 163–165]. Since the relating work requires considerable expertise in Material Science, we do not elaborate any further. *That said, the improvement of the printing system based on a thorough understanding of the process remains the most general solution for the promotion of AM in engineering practice.*

5.3 Performance Verification for Product Use

In spite of the establishment of quality control by minimizing the undesirable properties, mechanical testing has also been frequently carried out to determine the *material properties* of the printed part and to evaluate the *residual stress* distribution, both of which are fundamental to predict the service performance of end-use parts. Although the demand is quite immediate, a testing standard for AM parts is yet to be available.

At the current stage, tensile/compression testing is still the most extensively employed technique to characterize the material constitutive behaviour. In pursuit of the elasto-plastic properties, it is routine to print a group of specimens along with the workpiece. Due to the nature of anisotropy and low repeatability in AM, these specimens are required to be printed in different directions and each with several duplicates (Fig. 28). The number of specimens, as a consequence, is considerably large and the performance verification of AM fabricated part can be less cost-effective, taking at the meantime the relatively high price of the metal powder into account.[6] Furthermore, since the material properties obtained from tests such as tensile testing are somewhat global, it seems unsound to generalize these averaged values over the part since the distribution of these properties is spatially uneven.

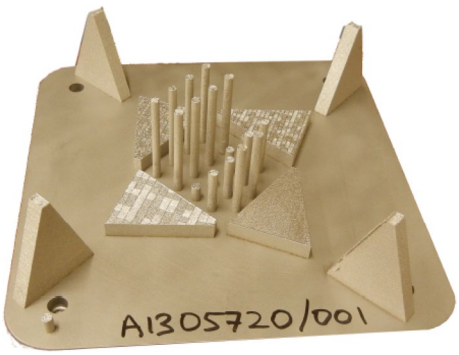

Fig. 28 Schematic of cylinder specimens for tensile testing and prism specimens for residual stress evaluation [143]

As for the estimation of RS, numerous techniques are now accessible and a systematic review is found in [167]. The so-called destructive methods deliberately remove material for the purpose of relaxation and redistribution of stresses. Popular methods within this regime include curvature methods, hole drilling, and compliance methods. Their gravest defect is the irrecoverable alteration of the tested part, making the part impossible for later use. Other methods like electron diffraction, X-ray diffraction and Neutrons diffraction in reference to physical diffraction, as well as magnetic and thermal-elastic methods are non-destructive ones. Their applications, however, have been restricted by their relatively high cost.

With all these in mind, we suggest that the mechanical tests should be performed on such a small scale (without breaking the tested part) that still assures the stimulation of a complex stress state to fully capture the material's *local* plastic behaviour. The instrumented indentation test (IIT), given its non-destructive nature[7] and the capacity for estimating

[6] The titanium metal powder, for example, can cost about $200–400 per kilogram as reported in [166].

[7] Compared to destructive tesings such as tensile test, IIT is considered non-destructive since the induced plastic deformation on the specimen is within the micron range.

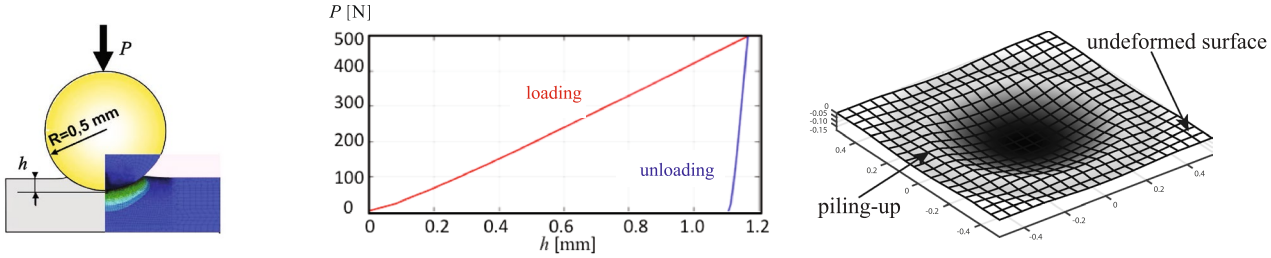

(a) Schematic of indentation test **(b)** Load-displacement (*P*-*h*) curve **(c)** Residual imprint

Fig. 29 Instrumented indentation test provides another option to locally and non-destructively characterize the mechanical properties and the residual stress on the printed part: **a** a schematic of the set up, **b** the resulting indentation curve and **c** the residual plastic deformation upon indenter removal [168]

local properties, promises an exciting solution for this problem [168–170]. It has rapidly become an alternative to conventional testing for material property characterization.

Similar to a standard hardness test [171], one forces during the indentation test a special indenter into the material surface by increasing the applied load until a user-defined load/displacement value; then the load is either held constant for a short duration before removal or immediately removed. The difference, compared with a hardness test, is that we continuously record the indentation force P and the indenter displacement h during both the loading and unloading phases, generating what we call an indentation (P–h) curve by the end of the test. Recently, high-precision measurement systems have led to a massive leap in the examination of experimental data, and the surface of the specimen can be scanned by such facilities as atomic force microscope (AFM) or confocal laser microscope (CLM). The advance in the measuring system has provided experimentalists with more information about material behaviour. Our previous work has revealed that the employment of the residual imprint has helped to gain some insights on the physical mechanism behind indentation, and improved the reliability of the identified material parameters [168, 172, 173, 199]. In Fig. 29 we present such a representative residual imprint along with (a) a schematic for spherical indentation using an indenter of radius 0.5 mm and (b) the resulting P–h curve.

Together with the advances in numerical methods, IIT has become nowadays an indispensable tool for probing mechanical properties. Its successful applications have been achieved not just for metals and alloys but also for ceramics [174], hydrated nano-composites such as concrete [175], polymers [176], single crystals [177] and plastically graded materials[178, 179]. Recently, Zeng et al. [180] has employed IIT to study the influence of the forming process on material properties. With this increasing maturity, IIT has also been adopted for the estimation of RS, inspired by the fact that both the indentation work and the residual pile-up are sensitive to residual stresses [181]. Leading research in this direction is found in [182, 183].

Unfortunately, we note that, for the time being, indentation has been preliminarily employed to study the hardness of the AM parts, while neither the plasticity nor the RS has been evaluated by this means. Since the merits being so prominent, the application of IIT for AM parts is envisaged to explode dramatically, and we are confident that this technique will bring the low-cost characterization of the built part into reality in the near future.

6 Conclusion

In this paper, we briefly reviewed both the topology optimization methodologies and the cutting-edge additive manufacturing techniques. Successful applications in the two directions were first cited respectively. An illustrative example of the aerospace bracket was further provided to promote the understanding of how AM and TO can be used synergistically for design and manufacturing. With a particular interest in the printing of critical parts, we also discussed in-depth the many challenges that have emerged upon the combination of TO and AM, regardless of their prominent advantages in the sense of weight competitiveness and salient flexibility. For future study, the following research directions are identified:

a. More advanced topology optimization methods need to be developed in responding to the urgent need for multi-functional and monolithic products. Preliminary study along this direction can be found in [184]. The challenge to be addressed is the compromise between the unity of the component and its ease of manufacturability, with the removal of supporting structures in mind.
b. To promote the structural performance to a higher level, another direction deserving more attention is the multi-scale topology optimization, in which the macro structure is optimized concurrently with local materials at the microscopic scale. Pioneering work is referred in [27–29, 185].

c. New protocols to design lightweight cellular material structures are in great demand for high performance and multi-functionality. Promising results have been widely reported for benchmark flat sandwich panels [186, 187], and designs of lattice structures [188–190].
d. The speed and resolution of the fabrication need to be further enhanced. Current improvement in the mechanical system consists of introducing two more rotation axes, which leads not only to the acceleration of the printing, but also to the elimination of support structures [191, 192]. Further research to incorporate with this improvement includes the slicing optimization and scanning pattern design [193, 194].
e. The instrumented indentation test proposed in Sect. 5.3, despite being non-destructive, requires the preparation of specimens. Fortunately, the current situation is now being changed by researchers from the LGCGM group from Université de Rènnes 1, France, who have presented an in-situ IIT system at the Industrie Paris on March 2018. However, continuing efforts are still needed to assess material performances on parts and to ascertain the components' performance in service [195–197]. On the other hand, due to the non-uniqueness issue related to the inverse identification (previously studied in [173, 198, 199]), the reliability of the derived material properties needs to be further verified.

That said, we insist on a long-term partnership to be cultivated between topology optimization and additive manufacturing, and their combination is envisaged to lead to establishing a further specialised design and manufacturing industry.

Acknowledgements The first author would like to give special thanks to Liang Xia, from Huazhong University of Science and Technology, China, who worked closely with the author on every step of the research and helped to bring the article into its current shape. We would also like to thank Caroline Verdari and Jing Wen, from Université de Technologie de Compiègne, France, for their kind help with the preparation of the indentation specimens. The financial support from the National Key Research and Development Program of China (2017YFB1102800), the National Natural Science Foundation of China (11672239, 51735005, 11620101002) is also acknowledged. This work has also been supported by the French National Research Agency (ANR) through the research grant Micromorfing, ANR-14-CE07-0035-01.

Compliance with Ethical Standards

Conflict of interest The authors declare that they have no conflict of interest.

References

1. Duysinx P, Bendsøe MP (1998) Topology optimization of continuum structures with local stress constraints. Int J Numer Methods Eng 43(8):1453
2. Allaire G, Jouve F, Maillot H (2004) Topology optimization for minimum stress design with the homogenization method. Struct Multidiscip Optim 28(2–3):87
3. Meng L, Zhang WH, Zhu JH, Xu Z, Cai SH (2016) Shape optimization of axisymmetric solids with the finite cell method using a fixed grid. Acta Mech Sin 32:510
4. Bendsoe MP, Sigmund O (2013) Topology optimization: theory, methods, and applications. Springer, Berlin
5. Zhang W, Sun S (2006) Scale-related topology optimization of cellular materials and structures. Int J Numer Methods Eng 68(9):993
6. Huang X, Xie M (2010) Evolutionary topology optimization of continuum structures: methods and applications. Wiley, New York
7. Xu Y, Zhu J, Wu Z, Cao Y, Zhao Y, Zhang W (2018) A review on the design of laminated composite structures: constant and variable stiffness design and topology optimization. Adv Compos Hybrid Mater 1–18
8. Rozvany GI (2009) A critical review of established methods of structural topology optimization. Struct Multidiscip Optim 37(3):217
9. Zhu JH, Zhang WH, Xia L (2016) Topology optimization in aircraft and aerospace structures design. Arch Comput Methods Eng 23(4):595
10. Liu J, Gaynor AT, Chen S, Kang Z, Suresh K, Takezawa A, Li L, Kato J, Tang J, Wang CC et al (2018) Current and future trends in topology optimization for additive manufacturing. Struct Multidiscip Optim 1–27
11. Gao T, Zhang W (2010) Topology optimization involving thermo-elastic stress loads. Struct Multidiscip Optim 42(5):725
12. Zhu J, Zhang W, Beckers P (2009) Integrated layout design of multi-component system. Int J Numer Methods Eng 78(6):631
13. Zhu J, Zhang W (2010) Integrated layout design of supports and structures. Comput Methods Appl Mech Eng 199(9–12):557
14. Zhou Y, Zhang W, Zhu J, Xu Z (2016) Feature-driven topology optimization method with signed distance function. Comput Methods Appl Mech Eng 310:1
15. Bruggi M, Duysinx P (2012) Topology optimization for minimum weight with compliance and stress constraints. Struct Multidiscip Optim 46(3):369
16. Zhang W, Zhou Y, Zhu J (2017) A comprehensive study of feature definitions with solids and voids for topology optimization. Comput Methods Appl Mech Eng 325:289
17. París J, Navarrina F, Colominas I, Casteleiro M (2009) Topology optimization of continuum structures with local and global stress constraints. Struct Multidiscip Optim 39(4):419
18. Cai S, Zhang W (2015) Stress constrained topology optimization with free-form design domains. Comput Methods Appl Mech Eng 289:267
19. Liu H, Zhang W, Gao T (2015) A comparative study of dynamic analysis methods for structural topology optimization under harmonic force excitations. Struct Multidiscip Optim 51(6):1321
20. Zhang W, Zhong W, Guo X (2014) An explicit length scale control approach in simp-based topology optimization. Comput Methods Appl Mech Eng 282:71
21. Allaire G, Jouve F, Michailidis G (2016) Thickness control in structural optimization via a level set method. Struct Multidiscip Optim 53(6):1349
22. Harzheim L, Graf G (2006) A review of optimization of cast parts using topology optimization. Struct Multidiscip Optim 31(5):388
23. Xia Q, Shi T, Wang MY, Liu S (2010) A level set based method for the optimization of cast part. Struct Multidiscip Optim 41(5):735
24. Xia Q, Shi T, Wang MY, Liu S (2011) Simultaneous optimization of cast part and parting direction using level set method. Struct Multidiscip Optim 44(6):751

25. Lu J, Chen Y (2012) Manufacturable mechanical part design with constrained topology optimization. Proc Inst Mech Eng Part B J Eng Manuf 226(10):1727
26. Gebisa A, Lemu H (2017) Design for manufacturing to design for additive manufacturing: analysis of implications for design optimality and product sustainability. Procedia Manuf 13:724
27. Xia L, Breitkopf P (2014) Concurrent topology optimization design of material and structure within fe2 nonlinear multiscale analysis framework. Comput Methods Appl Mech Eng 278:524
28. Xia L, Breitkopf P (2015) Multiscale structural topology optimization with an approximate constitutive model for local material microstructure. Comput Methods Appl Mech Eng 286:147
29. Xia L, Breitkopf P (2017) Recent advances on topology optimization of multiscale nonlinear structures. Arch Comput Methods Eng 24(2):227
30. Da D, Yvonnet J, Xia L, Le MV, Li G (2018) Topology optimization of periodic lattice structures taking into account strain gradient. Comput Struct 210:28–40
31. Wang Y, Xu H, Pasini D (2017) Multiscale isogeometric topology optimization for lattice materials. Comput Methods Appl Mech Eng 316:568
32. Liu S, Li Q, Chen W, Tong L, Cheng G (2015) An identification method for enclosed voids restriction in manufacturability design for additive manufacturing structures. Front Mech Eng 10(2):126
33. Zhou L, Zhang W (2018) Topology optimization method considering structural connectivity for additive manufacturing with void features. Struct Multidiscip Optim (under revision)
34. Gaynor AT, Guest JK (2016) Topology optimization considering overhang constraints: eliminating sacrificial support material in additive manufacturing through design. Struct Multidiscip Optim 54(5):1157
35. Mass Y, Amir O (2017) Topology optimization for additive manufacturing: accounting for overhang limitations using a virtual skeleton. Addit Manuf 18:58
36. Wu AS, Brown DW, Kumar M, Gallegos GF, King WE (2014) An experimental investigation into additive manufacturing-induced residual stresses in 316l stainless steel. Metall Mater Trans A 45(13):6260
37. Kohn RV, Strang G (1986) Optimal design and relaxation of variational problems, i. Commun Pure Appl Math 39(1):113
38. Bendsøe MP, Kikuchi N (1988) Generating optimal topologies in structural design using a homogenization method. Comput Methods Appl Mech Eng 71(2):197
39. Bendsøe MP (1989) Optimal shape design as a material distribution problem. Struct Optim 1(4):193
40. Andreassen E, Clausen A, Schevenels M, Lazarov BS, Sigmund O (2011) Efficient topology optimization in matlab using 88 lines of code. Struct Multidiscip Optim 43(1):1
41. Sigmund O (2001) A 99 line topology optimization code written in matlab. Struct Multidiscip Optim 21(2):120
42. Sigmund O, Maute K (2013) Topology optimization approaches. Struct Multidiscip Optim 48(6):1031
43. Sigmund O (2007) Morphology-based black and white filters for topology optimization. Struct Multidiscip Optim 33(4–5):401
44. Xie YM, Steven GP (1993) A simple evolutionary procedure for structural optimization. Comput Struct 49(5):885
45. Querin O, Young V, Steven G, Xie Y (2000) Computational efficiency and validation of bi-directional evolutionary structural optimisation. Comput Methods Appl Mech Eng 189(2):559
46. Huang X, Xie YM (2010) A further review of eso type methods for topology optimization. Struct Multidiscip Optim 41(5):671
47. Abdi M, Wildman R, Ashcroft I (2014) Evolutionary topology optimization using the extended finite element method and isolines. Eng Optim 46(5):628
48. Da D, Xia L, Li G, Huang X (2018) Evolutionary topology optimization of continuum structures with smooth boundary representation. Struct Multidiscip Optim 57(6):2143
49. Sigmund O, Petersson J (1998) Numerical instabilities in topology optimization: a survey on procedures dealing with checkerboards, mesh-dependencies and local minima. Struct Optim 16(1):68
50. Zhou M, Shyy Y, Thomas H (2001) Checkerboard and minimum member size control in topology optimization. Struct Multidiscip Optim 21(2):152
51. Li Q, Steven G, Xie Y (2001) A simple checkerboard suppression algorithm for evolutionary structural optimization. Struct Multidiscip Optim 22(3):230
52. van Dijk NP, Maute K, Langelaar M, Van Keulen F (2013) Level-set methods for structural topology optimization: a review. Struct Multidiscip Optim 48(3):437
53. Zhu J, Zhao Y, Zhang W, Gu X, Gao T, Kong J, Shi G, Xu Y, Quan D (2019) Bio-inspired feature-driven topology optimization for rudder structure design. Eng Sci. https://doi.org/10.30919/es8d716
54. Zhang W, Zhao L, Gao T, Cai S (2017) Topology optimization with closed b-splines and boolean operations. Comput Methods Appl Mech Eng 315:652
55. Guo X, Zhang W, Zhong W (2014) Doing topology optimization explicitly and geometrically—a new moving morphable components based framework. J Appl Mech 81(8):081009
56. Zhang W, Chen J, Zhu X, Zhou J, Xue D, Lei X, Guo X (2017) Explicit three dimensional topology optimization via moving morphable void (mmv) approach. Comput Methods Appl Mech Eng 322:590
57. Xie X, Wang S, Xu M, Wang Y (2018) A new isogeometric topology optimization using moving morphable components based on r-functions and collocation schemes. Comput Methods Appl Mech Eng 339:61
58. Sokołowski J, Żochowski A (2001) Encyclopedia of optimization, Springer, pp 2625–2626
59. Bourdin B, Chambolle A (2003) Design-dependent loads in topology optimization, ESAIM: control. Optim Calc Var 9:19
60. Gao T, Qiu L, Zhang W (2017) Topology optimization of continuum structures subjected to the variance constraint of reaction forces. Struct Multidiscip Optim 56(4):755
61. Zhang W, Yang J, Xu Y, Gao T (2014) Topology optimization of thermoelastic structures: mean compliance minimization or elastic strain energy minimization. Struct Multidiscip Optim 49(3):417
62. Stanford B, Beran P (2012) Optimal compliant flapping mechanism topologies with multiple load cases. J Mech Des 134(5):051007
63. Wang MY, Chen S, Wang X, Mei Y (2005) Design of multimaterial compliant mechanisms using level-set methods. J Mech Des 127(5):941
64. Zhu JH, Li Y, Zhang WH, Hou J (2016) Shape preserving design with structural topology optimization. Struct Multidiscip Optim 53(4):893
65. Wang ZP, Poh LH, Dirrenberger J, Zhu Y, Forest S (2017) Isogeometric shape optimization of smoothed petal auxetic structures via computational periodic homogenization. Comput Methods Appl Mech Eng 323:250
66. Wang ZP, Turteltaub S (2015) Isogeometric shape optimization for quasi-static processes. Int J Numer Methods Eng 104:347
67. Collet M, Bruggi M, Duysinx P (2017) Topology optimization for minimum weight with compliance and simplified nominal stress constraints for fatigue resistance. Struct Multidiscip Optim 55(3):839
68. Le C, Norato J, Bruns T, Ha C, Tortorelli D (2010) Stress-based topology optimization for continua. Struct Multidiscip Optim 41(4):605

69. Holmberg E, Torstenfelt B, Klarbring A (2013) Stress constrained topology optimization. Struct Multidiscip Optim 48(1):33
70. Díaaz AR, Kikuchi N (1992) Solutions to shape and topology eigenvalue optimization problems using a homogenization method. Int J Numer Methods Eng 35(7):1487
71. He W, Bindel D, Govindjee S (2009) Topology optimization in microelectromechanical resonator design, Department of Civil and Environmental Engineering, University of California
72. Ma ZD, Kikuchi N, Cheng HC (1995) Topological design for vibrating structures. Comput Methods Appl Mech Eng 121(1–4):259
73. Jog C (2002) Topology design of structures subjected to periodic loading. J Sound Vib 253(3):687
74. Zhang W, Liu H, Gao T (2015) Topology optimization of large-scale structures subjected to stationary random excitation: an efficient optimization procedure integrating pseudo excitation method and mode acceleration method. Comput Struct 158:61
75. Li Q, Steven GP, Xie Y (2001) Thermoelastic topology optimization for problems with varying temperature fields. J Therm Stress 24(4):347
76. Xia Q, Wang MY (2008) Topology optimization of thermoelastic structures using level set method. Comput Mech 42(6):837
77. Pedersen P, Pedersen NL (2010) Strength optimized designs of thermoelastic structures. Struct Multidiscip Optim 42(5):681
78. Michailidis G (2014) Manufacturing constraints and multi-phase shape and topology optimization via a level-set method. Ph.D. thesis, Ecole Polytechnique X
79. Zhou M, Fleury R, Shyy YK, Thomas H, Brennan J (2002) 9th AIAA/ISSMO symposium on multidisciplinary analysis and optimization, p 5614
80. Krog L, Tucker A, Rollema G (2002) Proceedings of 3rd Altair UK HyperWorks users Conference
81. Krog L, Tucker A, Kemp M, Boyd R (2004) 10th AIAA/ISSMO multidisciplinary analysis and optimization conference, p 4481
82. Kono D, Nishio S, Yamaji I, Matsubara A (2015) A method for stiffness tuning of machine tool supports considering contact stiffness. Int J Mach Tools Manuf 90:50
83. Liu H, Jiakun W, Yongqing W (2015) Impact of anchor bolts creep relaxation on geometric accuracy decline of large computer numerical control machine tools. J Xi'an Jiaotong Univ 49(9):14
84. Mahdavi A, Balaji R, Frecker M, Mockensturm E (2006) Topology optimization of 2d continua for minimum compliance using parallel computing. Struct Multidiscip Optim 32(2):121
85. Brandt M, Sun SJ, Leary M, Feih S, Elambasseril J, Liu QC (2013) Advanced materials research, vol 633, Trans Tech Publ, pp 135–147
86. Beaman JJ, Deckard CR (1990) Selective laser sintering with assisted powder handling. US Patent 4,938,816
87. Herzog D, Seyda V, Wycisk E, Emmelmann C (2016) Additive manufacturing of metals. Acta Mater 117:371
88. State-of-the-art for additive manufacturing of metals (2017). URLhttp://www.metalliskamaterial.se/globalassets/3-forskning/rapporter/2016-03898---state-of-the-art-for-additive-manufacturing-of-metals-2_1.pdf
89. Shellabear M, Nyrhilä O (2004) Dmls-development history and state of the art. Laser Assisted Netshape engineering 4, proceedings of the 4th LANE, pp 21–24
90. Calignano F, Manfredi D, Ambrosio E, Iuliano L, Fino P (2013) Influence of process parameters on surface roughness of aluminum parts produced by dmls. Int J Adv Manuf Technol 67(9–12):2743
91. Frazier WE (2014) Metal additive manufacturing: a review. J Mater Eng Perform 23(6):1917
92. Brandl E, Palm F, Michailov V, Viehweger B, Leyens C (2011) Mechanical properties of additive manufactured titanium (ti–6al–4v) blocks deposited by a solid-state laser and wire. Mater Des 32(10):4665
93. Crivello JV, Reichmanis E (2013) Photopolymer materials and processes for advanced technologies. Chem Mater 26(1):533
94. Guo N, Leu MC (2013) Additive manufacturing: technology, applications and research needs. Front Mech Eng 8(3):215
95. Wilkes J, Hagedorn YC, Meiners W, Wissenbach K (2013) Additive manufacturing of zro2–al2o3 ceramic components by selective laser melting. Rapid Prototyp J 19(1):51
96. Deckers J, Vleugels J, Kruth JP (2014) Additive manufacturing of ceramics: a review. J Ceram Sci Technol 5(4):245
97. Agrawal BK (1988) Introduction to engineering materials. Tata McGraw-Hill Education, New York
98. Badrossamay M, Childs T (2007) Further studies in selective laser melting of stainless and tool steel powders. Int J Mach Tools Manuf 47(5):779
99. Abd-Elghany K, Bourell D (2012) Property evaluation of 304l stainless steel fabricated by selective laser melting. Rapid Prototyp J 18(5):420
100. Kempen K, Yasa E, Thijs L, Kruth JP, Van Humbeeck J (2011) Microstructure and mechanical properties of selective laser melted 18ni-300 steel. Phys Procedia 12:255
101. Cormier D, Harrysson O, West H (2004) Characterization of h13 steel produced via electron beam melting. Rapid Prototyp J 10(1):35
102. Snoxall N (2018) Titanium challenge-design proposal. https://altairuniversity.com/wp-content/uploads/2013/09/Design-Proposal-Altair.pdf. Accessed 1 Aug 2018
103. Tan X, Kok Y, Tan YJ, Descoins M, Mangelinck D, Tor SB, Leong KF, Chua CK (2015) Graded microstructure and mechanical properties of additive manufactured ti–6al–4v via electron beam melting. Acta Mater 97:1
104. Baufeld B, Brandl E, Van der Biest O (2011) Wire based additive layer manufacturing: comparison of microstructure and mechanical properties of ti–6al–4v components fabricated by laser-beam deposition and shaped metal deposition. J Mater Process Technol 211(6):1146
105. Vilaro T, Colin C, Bartout JD (2011) As-fabricated and heat-treated microstructures of the ti–6al–4v alloy processed by selective laser melting. Metall Mater Trans A 42(10):3190
106. Brice C, Shenoy R, Kral M, Buchannan K (2015) Precipitation behavior of aluminum alloy 2139 fabricated using additive manufacturing. Mater Sci Eng A 648:9
107. Yang KK, Zhu JH, Wang C, Jia DS, Song LL, Zhang WH (2018) Experimental validation of 3d printed material behaviors and their influence on the structural topology design. Comput Mech 61(5):581–598
108. Yuan S, Shen F, Chua CK, Zhou K (2018) Polymeric composites for powder-based additive manufacturing: Materials and applications. Prog Polym Sci
109. Yuan S, Zheng Y, Chua CK, Yan Q, Zhou K (2018) Electrical and thermal conductivities of mwcnt/polymer composites fabricated by selective laser sintering. Compos Part A Appl Sci Manuf 105:203
110. Stratasys (2014) Direct digital manufacturing at bmw (January 15, 2014). URLhttp://3dprinting.trimech.com/case-study-fdm-bmw
111. Jauhar S, Asthankar K, Kuthe A (2012) Cost benefit analysis of rapid manufacturing in automotive industries. Adv Mech Eng Appl (AMEA) 2(3):181
112. Center FM (2014) Ford 3d-printed auto parts save millions, boost quality. URLhttps://www.plasticstoday.com/content/ford-3d-printed-auto-parts-save-millions-boost-quality/97214356120060
113. Fleming J (2018) Additive manufacturing in the automotive industry: insights from ford and bmw (September 15, 2018).

URLhttps://generisgp.com/2018/01/02/additive-manufacturing-automotive-ford-bmw/
114. Press DU (2018) 3d opportunity in the automotive undustry—additive manufacturing hits the road (September 15, 2018). URLhttps://www2.deloitte.com/content/dam/insights/us/articles/additive-manufacturing-3d-opportunity-in-automotive/DUP_707-3D-Opportunity-Auto-Industry_MASTER.pdf
115. D. printing industry (2018) Volkswagen to mass customise 100,000 3d printed units per year using the newly launched hp metal jet 3d printer (September 14, 2018). URLhttps://spare-parts-3d.com/2018/09/14/vw-customise-100000-3d-printed-hp-metal-jet/
116. ENGINEER (2018) Bmw group to invest over 10 m €in new additive manufacturing campus (April 18, 2018). URLhttps://www.theengineer.co.uk/bmw-group-additive-manufacturing-campus/
117. Tomlin M, Meyer J (2011) Proceeding of the 7th altair CAE technology conference, pp 1–9
118. Machunze W, Lehmann T, Hein O (2013) 2013 European altair technology conference, pp 1–25
119. Snoxall N (2013) Topology optimization for additive manufacture: Titanium challenge—design proposal. URLhttps://altairuniversity.com/wp-content/uploads/2013/09/Design-Proposal-Altair.pdf
120. Sher D (2013) 5-m long titanium airplane part 3d printed in one piece (January 18, 2013). URLhttps://www.3ders.org/articles/20130118-3-meter-long-titanium-airplane-part-3d-printed-in-one-piece.html
121. Sher D (2018) Ge aviation already 3d printed 30,000 fuel nozzles for its leap engine (October 5, 2018). URLhttps://www.3dprintingmedia.network/ge-aviation-already-3d-printed-30000-fuel-nozzles-for-its-leap-engine/
122. Tripathy S (2016) Topology optimization for additive manufacturing applications. http://blogs.3ds.com/simulia/topology-optimization-for-additive-manufacturing-applications/. Accessed 23 Aug 2016
123. EOS (2018) Aerospace: Ruag-additive manufacturing of satellite components (September 15, 2018). URLhttps://www.eos.info/case_studies/additive-manufacturing-of-antenna-bracket-for-satellite
124. EOS (2018) Eos and airbus group innovations team on aerospace sustainability study for industrial 3d printing. https://www.eos.info/eos-airbusgroupinnovationteam-aerospace-sustainability-study. Accessed 31 June 2018
125. Kranz J, Herzog D, Emmelmann C (2015) Design guidelines for laser additive manufacturing of lightweight structures in ti–al6–v4. J Laser Appl 27(S1):S14001
126. Zelinski P (2016) 7 Helpful numbers quantify design rules for additive manufacturing. URLhttps://www.additivemanufacturing.media/blog/post/7-helpful-numbers-quantify-design-rules-for-am
127. Hu K, Jin S, Wang CC (2015) Support slimming for single material based additive manufacturing. Comput Aided Des 65:1
128. Morgan H, Cherry J, Jonnalagadda S, Ewing D, Sienz J (2016) Part orientation optimisation for the additive layer manufacture of metal components. Int J Adv Manuf Technol 86(5–8):1679
129. Pandey PM, Thrimurthulu K, Reddy NV (2004) Optimal part deposition orientation in fdm by using a multicriteria genetic algorithm. Int J Prod Res 42(19):4069
130. Phatak AM, Pande S (2012) Optimum part orientation in rapid prototyping using genetic algorithm. J Manuf Syst 31(4):395
131. Huang X, Ye C, Wu S, Guo K, Mo J (2009) Sloping wall structure support generation for fused deposition modeling. Int J Adv Manuf Technol 42(11–12):1074
132. Vanek J, Galicia JAG, Benes B (2014) Computer graphics forum, vol 33, Wiley Online Library, pp 117–125
133. Mezzadri F, Bouriakov V, Qian X (2018) Topology optimization of self-supporting support structures for additive manufacturing. Addit Manuf 21:666
134. Dumas J, Hergel J, Lefebvre S (2014) Bridging the gap: automated steady scaffoldings for 3d printing. ACM Trans Gr (TOG) 33(4):98
135. Barnett E, Gosselin C (2015) Weak support material techniques for alternative additive manufacturing materials. Addit Manuf 8:95
136. Brackett D, Ashcroft I, Hague R (2011) Proceedings of the solid freeform fabrication symposium, Austin, TX, vol 1, pp 348–362
137. Zhang W, Zhou L (2018) Topology optimization of self-supporting structures with polygon features for additive manufacturing. Comput Methods Appl Mech Eng 334:56
138. Meyer B, Minn E (2016) Accuracy in additive manufacturing. Mach Des 84:56
139. Murr LE, Gaytan S, Ceylan A, Martinez E, Martinez J, Hernandez D, Machado B, Ramirez D, Medina F, Collins S et al (2010) Characterization of titanium aluminide alloy components fabricated by additive manufacturing using electron beam melting. Acta Mater 58(5):1887
140. Press DU (2018) Ultrasonic additive manufacturing (September 15, 2018). URLhttps://fabrisonic.com/ultrasonic-additive-manufacturing-overview/
141. Murr LE, Gaytan SM, Ramirez DA, Martinez E, Hernandez J, Amato KN, Shindo PW, Medina FR, Wicker RB (2012) Metal fabrication by additive manufacturing using laser and electron beam melting technologies. J Mater Sci Technol 28(1):1
142. Mower TM, Long MJ (2016) Mechanical behavior of additive manufactured, powder-bed laser-fused materials. Mater Sci Eng A 651:198
143. Tripathy S, Chin C, London T, Ankalkhope U, Oancea V (2017) Process modeling and validation of powder bed metal additive manufacturing. In: NAFEMS world congress, Stockholm, Sweden
144. Wu X, Liang J, Mei J, Mitchell C, Goodwin P, Voice W (2004) Microstructures of laser-deposited ti–6al–4v. Mater Des 25(2):137
145. Mok SH, Bi G, Folkes J, Pashby I (2008) Deposition of ti–6al–4v using a high power diode laser and wire, part i: investigation on the process characteristics. Surf Coat Technol 202(16):3933
146. Zhu Y, Tian X, Li J, Wang H (2015) The anisotropy of laser melting deposition additive manufacturing ti–6.5 al–3.5 mo–1.5 zr–0.3 si titanium alloy. Mater Des 67:538
147. Brandl E, Baufeld B, Leyens C, Gault R (2010) Additive manufactured ti–6al–4v using welding wire: comparison of laser and arc beam deposition and evaluation with respect to aerospace material specifications. Phys Procedia 5(Pt 2):595
148. Baufeld B (2012) Effect of deposition parameters on mechanical properties of shaped metal deposition parts. Proc Inst Mech Eng Part B J Eng Manuf 226(1):126
149. Kruth JP, Mercelis P, Van Vaerenbergh J, Froyen L, Rombouts M (2005) Binding mechanisms in selective laser sintering and selective laser melting. Rapid Prototyp J 11(1):26
150. Thijs L, Verhaeghe F, Craeghs T, Van Humbeeck J, Kruth JP (2010) A study of the microstructural evolution during selective laser melting of ti–6al–4v. Acta Mater 58(9):3303
151. Papadakis L, Loizou A, Risse J, Bremen S, Schrage J (2014) A computational reduction model for appraising structural effects in selective laser melting manufacturing: a methodical model reduction proposed for time-efficient finite element analysis of larger components in selective laser melting. Virtual Phys Prototyp 9(1):17

152. Smith J, Xiong W, Yan W, Lin S, Cheng P, Kafka OL, Wagner GJ, Cao J, Liu WK (2016) Linking process, structure, property, and performance for metal-based additive manufacturing: computational approaches with experimental support. Comput Mech 57(4):583
153. Contuzzi N, Campanelli S, Ludovico A (2011) 3 d finite element analysis in the selective laser melting process. Int J Simul Model 10(3):113
154. Abe F, Osakada K, Shiomi M, Uematsu K, Matsumoto M (2001) The manufacturing of hard tools from metallic powders by selective laser melting. J Mater Process Technol 111(1–3):210
155. Alyoshin N, Murashov V, Grigoryev M, Yevgenov A, Karachevtsev F, Shchipakov N, Vasilenko S (2017) Defects of heat-resistant alloys synthesized by the method of selective laser melting. Inorg Mater Appl Res 8(1):27
156. Hussein A, Hao L, Yan C, Everson R (2013) Finite element simulation of the temperature and stress fields in single layers built without-support in selective laser melting. Mater Des 52:638
157. De A, DebRoy T (2006) Improving reliability of heat and fluid flow calculation during conduction mode laser spot welding by multivariable optimisation. Sci Technol Weld Join 11(2):143
158. Patterson AE, Messimer SL, Farrington PA (2017) Overhanging features and the slm/dmls residual stresses problem: review and future research need. Technologies 5(2):15
159. Kruth JP, Deckers J, Yasa E, Wauthlé R (2012) Assessing and comparing influencing factors of residual stresses in selective laser melting using a novel analysis method. Proc Inst Mech Eng Part B J Eng Manuf 226(6):980
160. Carter LN, Martin C, Withers PJ, Attallah MM (2014) The influence of the laser scan strategy on grain structure and cracking behaviour in slm powder-bed fabricated nickel superalloy. J Alloys Compd 615:338
161. Guan K, Wang Z, Gao M, Li X, Zeng X (2013) Effects of processing parameters on tensile properties of selective laser melted 304 stainless steel. Mater Des 50:581
162. Shiomi M, Osakada K, Nakamura K, Yamashita T, Abe F (2004) Residual stress within metallic model made by selective laser melting process. CIRP Ann Manuf Technol 53(1):195
163. Popovich V, Borisov E, Popovich A, Sufiiarov VS, Masaylo D, Alzina L (2017) Functionally graded inconel 718 processed by additive manufacturing: crystallographic texture, anisotropy of microstructure and mechanical properties. Mater Des 114:441
164. Carroll BE, Palmer TA, Beese AM (2015) Anisotropic tensile behavior of ti–6al–4v components fabricated with directed energy deposition additive manufacturing. Acta Mater 87:309
165. Murr L (2015) Metallurgy of additive manufacturing: examples from electron beam melting. Addit Manuf 5:40
166. Froes F, Friedrich H, Kiese J, Bergoint D (2004) Titanium in the family automobile: the cost challenge. JOM 56(2):40
167. Withers P, Bhadeshia H (2001) Residual stress. Part 1—measurement techniques. Mater Sci Technol 17(4):355
168. Meng L, Breitkopf P, Raghavan B, Mauvoisin G, Bartier O, Hernot X (2015) Identification of material properties using indentation test and shape manifold learning approach. Comput Methods Appl Mech Eng 297:239
169. Mott BW (1956) Micro-indentation hardness testing. Butterworths Scientific Publications, London
170. Tabor D (1951) The hardness of metals, vol 10. Clarendon Press, Oxford
171. Smith RL, Sandly GE (1922) An accurate method of determining the hardness of metals, with particular reference to those of a high degree of hardness. Proc Inst Mech Eng 102(1):623
172. Meng L, Breitkopf P, Le Quilliec G (2017) An insight into the identifiability of material properties by instrumented indentation test using manifold approach based on ph curve and imprint shape. Int J Solids Struct 106:13
173. Meng L, Breitkopf P, Raghavan B, Mauvoisin G, Bartier O, Hernot X (2018) On the study of mystical materials identified by indentation on power law and voce hardening solids. Int J Mater Form 1–16
174. Mukhopadhyay A (1999) Comparative study of indentation fatigue in structural ceramics. J Mater Sci Lett 18(4):333
175. Kamali-Bernard S, Keinde D, Bernard F (2014) Effect of aggregate type on the concrete matrix/aggregates interface and its influence on the overall mechanical behavior. A numerical study. Key Eng Mater 617:14
176. Lu Y, Shinozaki D (2005) Effects of substrate constraint on micro-indentation testing of polymer coatings. Mater Sci Eng A 396(1–2):77
177. Sabnis PA, Forest S, Arakere NK, Yastrebov VA (2013) Crystal plasticity analysis of cylindrical indentation on a ni-base single crystal superalloy. Int J Plast 51:200
178. Moy CK, Bocciarelli M, Ringer SP, Ranzi G (2011) Identification of the material properties of al 2024 alloy by means of inverse analysis and indentation tests. Mater Sci Eng A 529:119
179. Moussa C, Bartier O, Mauvoisin G, Hernot X, Collin JM, Delattre G (2014) Experimental and numerical investigation on carbonitrided steel characterization with spherical indentation. Surf Coat Technol 258:782
180. Zeng Y, Yu X, Wang H (2018) A new pod-based approximate Bayesian computation method to identify parameters for formed ahss. Int J Solids Struct 160:120–133
181. Chen X, Yan J, Karlsson AM (2006) On the determination of residual stress and mechanical properties by indentation. Mater Sci Eng A 416(1):139
182. Rickhey F, Lee JH, Lee H (2015) A contact size-independent approach to the estimation of biaxial residual stresses by knoop indentation. Mater Des 84:300
183. Shen L, He Y, Liu D, Gong Q, Zhang B, Lei J (2015) A novel method for determining surface residual stress components and their directions in spherical indentation. J Mater Res 30(08):1078
184. Wang X, Xu S, Zhou S, Xu W, Leary M, Choong P, Qian M, Brandt M, Xie YM (2016) Topological design and additive manufacturing of porous metals for bone scaffolds and orthopaedic implants: a review. Biomaterials 83:127
185. Collet M, Noël L, Bruggi M, Duysinx P (2018) Topology optimization for microstructural design under stress constraints. Struct Multidiscip Optim 58(6):2677–2695
186. Deshpande VS, Fleck NA, Ashby MF (2001) Effective properties of the octet-truss lattice material. J Mech Phys Solids 49(8):1747
187. Wallach J, Gibson L (2001) Mechanical behavior of a three-dimensional truss material. Int J Solids Struct 38(40–41):7181
188. Wang AJ, McDowell D (2003) Optimization of a metal honeycomb sandwich beam-bar subjected to torsion and bending. Int J Solids Struct 40(9):2085
189. Wang H, Chen Y, Rosen DW (2005) ASME 2005 international design engineering technical conferences and computers and information in engineering conference, American Society of Mechanical Engineers, pp 421–427
190. Yuan S, Chua CK, Zhou K (2018) 3d-printed mechanical metamaterials with high energy absorption. Adv Mater Technol 1800419
191. Doubrovski Z, Verlinden JC, Geraedts JM (2011) ASME 2011 international design engineering technical conferences and computers and information in engineering conference, American Society of Mechanical Engineers, pp 635–646
192. Eiamsa-ard K, Ruan J, Ren L, Liou FW (2005) ASME 2005 international design engineering technical conferences and computers and information in engineering conference, American Society of Mechanical Engineers, pp 1309–1319
193. Kanakanala D, Routhu S, Ruan J, Liu XF, Liou F (2010) ASME 2010 international design engineering technical conferences and

computers and information in engineering conference, American Society of Mechanical Engineers, pp 425–432
194. Routhu S, Kanakanala D, Ruan J, Liu XF, Liou F (2010) ASME 2010 international design engineering technical conferences and computers and information in engineering conference, American Society of Mechanical Engineers, pp 415–423
195. Hou Y, Sapanathan T, Dumon A, Culière P, Rachik M (2018) A novel development of bi-level reduced surrogate model to predict ductile fracture behaviors. Eng Fract Mech 188:232
196. Hou Y, Tie Y, Li C, Sapanathan T, Rachik M (2019) Low-velocity impact behaviors of repaired cfrp laminates: effect of impact location and external patch configurations. Compos Part B Eng 163:669
197. Idriss M, Bartier O, Mauvoisin G, Hernot X (2019) Determining the stress level of monotonic plastically pre-hardened metal sheets using the spherical instrumented indentation technique. J Mech Sci Technol 33(1):183
198. Chen X, Ogasawara N, Zhao M, Chiba N (2007) On the uniqueness of measuring elastoplastic properties from indentation: the indistinguishable mystical materials. J Mech Phys Solids 55(8):1618
199. Meng L, Raghavan B, Bartier O et al (2017) An objective metamodeling approach for indentation-based material characterization. Mech Mater 107:31–44